

**INVESTIGATING THE FILAMENT WOUND  
HYBRID CYLINDRICAL STRUCTURES WITH  
ENHANCED THERMAL PROPERTIES BY  
NUMERICAL ANALYSIS**

**A Thesis Submitted to  
the Graduate School of Engineering and Sciences of  
İzmir Institute of Technology  
in Partial Fulfillment of the Requirements for the Degree of**

**MASTER OF SCIENCE**

**in Mechanical Engineering**

**by  
Mert ÖZKAN**

**June 2023  
İZMİR**

We approve the thesis of **Mert ÖZKAN**

**Examining Committee Members:**

---

**Prof. Dr. Metin TANOĞLU**

Department of Mechanical Engineering, İzmir Institute of Technology

---

**Prof. Dr. Engin AKTAŞ**

Department of Civil Engineering, İzmir Institute of Technology

---

**Doç. Dr. Aylin ZİYLAN**

Department of Metallurgical and Materials Engineering, Dokuz Eylül University

**19 June 2023**

---

**Prof. Dr. Metin TANOĞLU**

Supervisor, Department of Mechanical Engineering, İzmir Institute of Technology

---

**Prof. Dr. Metin TANOĞLU**

Department of Mechanical Engineering, İzmir Institute of Technology

---

**Prof. Dr. Mehtap EANES**

Dean of the Graduate School of Engineering and Science

## ACKNOWLEDGMENTS

First of all, I would like to thank my thesis advisor Prof. Metin TANOĞLU for his understanding and support in every problem that I experienced. His guidance and patience allowed me to always find a new path in my master's study to solve the problem.

Additionally, thanks to the composite laboratories research group, who helped and supported me when I was not handle anything in my master's study, Dora ÖZARSLAN, Seçkin MARTİN, Ceren TÜRKDOĞAN DAMAR, Melisa YEKE, Kaan NUHOĞLU, Senagül TUNCA TAŞKIRAN, Ahmet Ayberk GÜRBÜZ, Nazife ÇERÇİ, Erdal ULAŞLI.

Also, I would like to thank my bosses Yusuf Can UZ and Okan BOSTAN for helping me with my master's studies and for supporting my studies even at the busiest times.

Finally, I would like to thank my family, my sister Gizem ÖZKAN ERDOĞAN, mother Aysun ÖZKAN and father Ayhan Akın ÖZKAN, for their supports throughout my life.

# ABSTRACT

## INVESTIGATING THE FILAMENT WOUND HYBRID CYLINDRICAL STRUCTURES WITH ENHANCED THERMAL PROPERTIES BY NUMERICAL ANALYSIS

The filament winding method is a composite production technique found at the beginning of the 20th century. The technique has been used in different fields since the day it was introduced in literature. Today, with the developments in the continuous fiber structure used in this technique and the development of carbon technology, filament-wound composites are widely used in the automotive, aerospace, and defense industries.

In this study, the finite element method was used to model filament-wound composite cylinders. It was wanted to observe the matrix effect of the composite structure numerically and criticize experimentally produced composites. Even though the current studies work on a hybridized composite structure with respect to the fiber, this study tried to find the hybridized matrix effect by numerical analysis. For this purpose, in this study, the finite element program ANSYS was used. In order to make realistic calculations with ANSYS, material data were observed from composite plates. Finite element models created with the obtained data were compared with the experimental results. The analysis results were observed with the help of the first-ply failure theory. In addition, since the pattern representations from the winding poles cannot be displayed in ANSYS, the pattern effect was ignored, and comparison were made with the assumption of a full layer at given angles.

As a result of all this study, although there were differences between experimental and finite element methods' models in homogeneity and pattern, methods' comparisons gave consistent and close results.

# ÖZET

## GELİŞTİRİLMİŞ TERMAL ÖZELLİKLERE SAHİP FİLAMAN SARGILI HİBRİT SİLİNDİRİK YAPILARIN SAYISAL ANALİZLE İNCELENMESİ

Filament sarma yöntemi ile kompozit silindir üretimi 20. Yüzyılın ilk çeyreğinden sonra keşfedilmiştir. Bu keşif sonrasında kapsamlı olarak çeşitli alanlarda yaygın bir şekilde kullanılmıştır. Günümüzde başlıca kullanım alanlarından olan havacılık ve uzay sanayiinde, karbon fiber teknolojisinin gelişmesiyle birlikte çalışmalara hız katmış; performans, üretilebilirlik, dayanım ve hafiflik açısından günümüz çalışmalarında daha yaygın bir kullanıma sahip olmuştur.

Bu çalışmada, hibrit yapının matris malzemesi ile oluşturulması amacı doğrultusunda, ıslak sarım esnasında farklı bir reçine ile üretilmiş katman kullanımının kompozit yapıya etkisi ve istenilen ek özelliklerin yapıya dahil edilebilmesinin mümkün ve işlevsel olup olmadığı sonlu eleman yöntemi ile tahmin edilmesi amaçlanmıştır. Güncel hibrit çalışmaları kompozit yapıdaki fiberler üzerine olsa da matris malzemesi ile oluşturulacak hibrit yapının yüksek ısıya dayanıklı bir reçinenin en dış katmanda kullanılarak altta kalan katmanlardaki yapıyı korumasının mümkün olup olmadığı gözlemlenmek istenmiştir. Gerçeğe yakın sonuçlar elde etmek amacıyla kullanılan fiber ve matris malzemelerinden kompozit plaka üretilip ANSYS'e işlenecek malzeme verileri bu plakalardan elde edilmiştir. Elde edilen malzeme verileri ile kompozit silindir yapıları program içerisinde modellenmiş ve analizleri gerçekleştirilmiştir. Gerçekleştirilen mekanik özellik testlerinin nümerik yöntemle tahmin edilmesi için "İlk Katman Kırılması" teorisi ve "Tersine Rezerv" faktörü kullanılmıştır.

Gerçekleştirilen analizler sonucunda, üretilen kompozit yapılar ile modellenen kompozit yapıların mekanik özelliklerin kıyas verileri elde edilmiştir. Elde edilen deneysel ve nümerik model sonuçları birbirleri ile kıyaslandığında, birbirleriyle yakın ve tutarlı değerleri verdiği ve kullanılan teorinin gelecek geliştirme çalışmalarına yardımcı olacağı gözlemlenmiştir.

# TABLE OF CONTENTS

LIST OF FIGURES .....	viii
LIST OF TABLES.....	xi
CHAPTER 1. INTRODUCTION .....	1
1.1. Introduction.....	1
1.2. Aim of thesis .....	2
1.3. Fundamentals of Composite Materials .....	3
1.3.1. Metal Matrix Composites (MMC's).....	4
1.3.2. Polymer Matrix Composites (PMC's).....	4
1.3.3. Ceramic Matrix Composites (CMC's) .....	5
1.4. Filament Winding Technique .....	6
1.5. Finite Element Method (FEM) Analysis.....	7
1.6. Thesis Outline .....	9
CHAPTER 2. LITERATURE SURVEY.....	10
CHAPTER 3. METHODOLOGY .....	30
3.1. Experimental .....	30
3.1.1. Materials .....	30
3.1.1.1. Fiber .....	30
3.1.1.2. Resin.....	31
3.1.2. Composite Structure Production.....	31
3.1.2.1. Composite Plate.....	32
3.1.2.2. Composite Cylinder .....	32
3.1.3. Test Methods .....	33
3.1.3.1. Plate Tests .....	33
3.1.3.1.1. Tensile Test.....	33
3.1.3.1.2. Combine Loading Test .....	34
3.1.3.1.3. V-Notch Beam Method .....	35

3.1.3.1.4. Thermal Conductivity.....	37
3.1.3.2. Composite Cylinder Tests.....	37
3.1.3.2.1. Three Point Bending.....	37
3.1.3.2.2. Hoop Tensile.....	39
3.1.3.2.3. Radial Compression.....	39
3.1.3.2.4. Thermal Test.....	40
3.2. Finite Element Method.....	40
3.2.1. Analysis Tree.....	41
3.2.2. ACP(PRE).....	42
3.2.3. Static Structural.....	42
3.2.4. Steady-State Thermal.....	43
3.2.5. ACP(POST).....	44
CHAPTER 4. RESULTS AND DISCUSSION.....	46
4.1. Material Properties.....	46
4.2. FEM Test Models and Results.....	49
4.2.1. Three Point Bending.....	49
4.2.2. Hoop Tensile.....	53
4.2.3. Radial Compression.....	56
4.2.4. Thermal Analysis.....	59
CHAPTER 5. CONCLUDING REMARKS.....	62
REFERENCES.....	64

# LIST OF FIGURES

<u>Figure</u>	<u>Page</u>
Figure 1. Schematic view of composite laminate structure. (Source: Potter, Kevin (1996).) .....	1
Figure 2. Filament winding technique (Source: Ma et al. 2019). .....	6
Figure 3. Comparison of the force-displacement result of mesh convergence (Source: Abdallah and Braimah 2022). .....	11
Figure 4. Tensile Stress-%elongation curves for Tube 1 (Source: Abdallah and Braimah 2022). .....	12
Figure 5. Tensile Stress-%elongation curves for Tube 2 (Source: Abdallah and Braimah 2022). .....	13
Figure 6. Load-Displacement curves for Tube 1 (Source: Abdallah and Braimah 2022). .....	13
Figure 7. Load-Displacement curves for Tube 2 (Source: Abdallah and Braimah 2022). .....	14
Figure 8. Moment application at both ends through insert contact surfaces (Source: Arslan Özgen et al., n.d.). .....	15
Figure 9. Torsional buckling analysis typical torsional buckling mode (Source: Arslan Özgen et al., n.d.). .....	16
Figure 10. Flowchart for iteration of suitable ply properties (Source: Toh et al. 2018). .....	17
Figure 11. Finite element models for the (a) uniaxial tensile test and (b) ring stiffness test (Source: Toh et al. 2018). .....	18
Figure 12. Force-displacement curve of the (a) uniaxial tensile test and (b) ring stiffness test (Source: Toh et al. 2018). .....	19
Figure 13. (a) Plot for hoop deformation; (b) Plot for axial stress; (c) Plot for hoop stress (Source: Gunasegaran, Prashanth, and Narayanan 2013). .....	22
Figure 14. Numerical damage modelling in Abaqus (Source: Maziz et al. 2021). .....	23
Figure 15. Boundary conditions of hybrid composite pipe (Source: Maziz et al. 2021). .....	24
Figure 16. Composite materials and stacking sequence (Source: Maziz et al. 2021). ....	25

<b><u>Figure</u></b>	<b><u>Page</u></b>
Figure 17. Predicted delamination according to the different stacking sequences through the thickness (Source: Maziz et al. 2021).....	25
Figure 18. Applied steps to find optimal parameters flow chart (Source: Zacharakis et al. 2022).....	27
Figure 19. Three-point bending pictures. (a) experimental model, (b) experimental maximum bending, (c) numerical model, (d) numerical maximum bending (Source: Zacharakis et al. 2022). ....	28
Figure 20. Ring test layup. (a) experimental model, (b) numerical model, (c) numerical test result (Source: Zacharakis et al. 2022). ....	28
Figure 21. A view of producing operation of composite plate. ....	32
Figure 22. A view of winding operation of composite cylinder. ....	33
Figure 23. A view of test specimen. ....	34
Figure 24. The Combined Loading Test Specimens.....	35
Figure 25. A view of V-Notch Beam test specimen. ....	36
Figure 26. KEM QTM 500 Thermal conductivity meter.....	37
Figure 27. Three-point bending test setup. ....	38
Figure 28. Hoop tensile test setup.....	39
Figure 29. Radial compression test setup. ....	40
Figure 30. An example analysis tree in ANSYS. ....	41
Figure 31. An example modelled composite structure in ACP(PRE). ....	42
Figure 32. Three-point bending test setup illustration.....	43
Figure 33. Thermal test demonstration. ....	44
Figure 34. Post processing image of the test setup. ....	44
Figure 35. Polar properties of composite structures. (a) Carbon/Epoxy, (b) Carbon/Phenolic.. ....	46
Figure 36. Three Point Bending test specimen technical drawing. ....	49
Figure 37. Three Point Bending analysis boundary conditions. (a) experimental, (b) front side FEM and (c) isometric view FEM.....	50
Figure 38. Three Point Bending FEM analyses stress results. (a) 5-layer Carbon/Epoxy pipe, (b) 4-layer Carbon/Epoxy and 1-layer Carbon/Phenolic composite pipe.....	51

<b><u>Figure</u></b>	<b><u>Page</u></b>
Figure 39. Three Point Bending FEM analyses failure analyses results. (a) 5-layer Carbon/Epoxy pipe, (b) 4-layer Carbon/Epoxy and 1-layer Carbon/Phenolic composite pipe. ....	52
Figure 40. Three Point Bending Analysis Stress-Strain graph. ....	52
Figure 41. Hoop Tensile test specimen technical drawing. ....	53
Figure 42. Hoop Tensile analysis boundary conditions. ....	53
Figure 43. Hoop Tensile FEM analyses stress results. (a) 5-layer Carbon/Epoxy pipe,(b) 4-layer Carbon/Epoxy and 1-layer Carbon/Phenolic composite pipe. ....	54
Figure 44. Hoop Tensile FEM analyses failure analyses results. (a) 5-layer Carbon/Epoxy pipe, (b) 4-layer Carbon/Epoxy and 1-layer Carbon/Phenolic composite pipe. ....	55
Figure 45. Hoop Tensile Analysis Stress-Strain graph. ....	55
Figure 46. Radial Compression test specimen technical drawing. ....	56
Figure 47. Radial compression analysis boundary conditions. ....	57
Figure 48. Radial Compression FEM analyses failure analyses results. (a) 5-layer Carbon/Epoxy pipe, (b) 4-layer Carbon/Epoxy and 1-layer Carbon/Phenolic composite pipe. ....	58
Figure 49. Radial Compression Analysis Stress-Strain graph. ....	58
Figure 50. Thermal boundary conditions of modelled analyses. ....	59
Figure 51. Thermal Conductivity FEM analyses failure analyses results. (a) 5-layer Carbon/Epoxy pipe, (b) 4-layer Carbon/Epoxy and 1-layer Carbon/Phenolic composite pipe. ....	60

# LIST OF TABLES

<b><u>Table</u></b>	<b><u>Page</u></b>
Table 1. Specifications of produced GFRP tubes (Source: Abdallah and Braimah 2022). .....	11
Table 2. Experimental results vs. numerical results for the Tube 1 and Tube 2 under radial compression test (Source: Abdallah and Braimah 2022). .....	12
Table 3. Stacking sequence of specimens (Source: Arslan Özgen et al., n.d.). .....	15
Table 4. FEM results for the torsional capacity and critical buckling torque of the specimens (Source: Arslan Özgen et al., n.d.). .....	16
Table 5. Test matrix and correspond standards (Source: Toh et al. 2018). .....	18
Table 6. List of variables (Source: Gunasegaran et al., 2013). .....	20
Table 7. L9 orthogonal array (Source: Gunasegaran, Prashanth, and Narayanan 2013). .....	20
Table 8. Magnitudes of control variables (Source: Gunasegaran, Prashanth, and Narayanan 2013). .....	21
Table 9. Nodal solutions for optimized pipes (Source: Gunasegaran, Prashanth, and Narayanan 2013). .....	22
Table 10. Geometry of the hybrid pipe (Source: Maziz et al. 2021). .....	24
Table 11. Tensile Test Specifications (Source: Zacharakis et al. 2022). .....	26
Table 12. The properties of DOWAKSA 12K A-49 continuous carbon fiber from data sheet. ....	31
Table 13. Fiber and resins viscosity and density properties. ....	31
Table 14. Composite materials' properties that are used in the ANSYS FEM program. ....	48
Table 15. Results of experimental test and finite element analysis. ....	61
Table 16. Differences and error rates of all methods and tests. ....	61

# CHAPTER 1

## INTRODUCTION

Composite materials are used in several industries because of new technologies' lightweight and resistivity needs. In order to achieve this goal, different production methods have been used for years. The filament winding technique used among these production methods has been the basis of this thesis. In this section, information about the basic points, objectives, methods, and general flow of the study is explained.

### 1.1. Introduction

Composite material, which has been used since times of old, is known as the material obtained by combining two or more materials (Clyne and Hull 2019). The main advantages of composite materials are their high strength-to-weight ratio, corrosion resistance, lightness, great mechanical properties, electrical and thermal insulation, and durability, which make composite materials an important part of the industry. Moreover, its manufacturability with the desired properties and strong applicability to the industry are other important topics (Chung 2010).

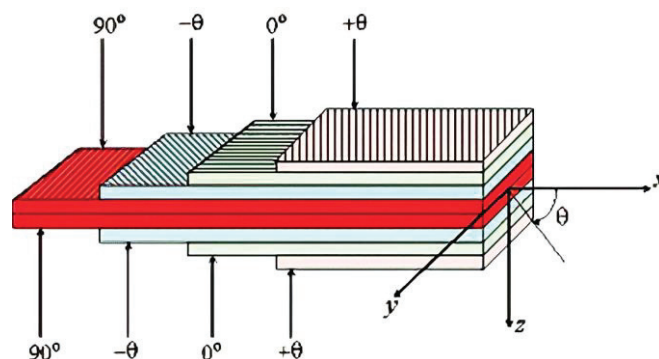


Figure 1. Schematic view of composite laminate structure. (Source: Potter, Kevin (1996).)

The history of composite materials dates back to ancient times when they were used as constructional materials. The bricks of the walls were produced by mixing mud and straw in a certain amount. The first examples that researchers mentioned are hunting equipment made from the Mongol and Egyptian pyramids' bricks (Šerifi 2018). The bows were made by using silk, bamboo, cattle tendons, and horns as reinforced materials; meanwhile, pine resin was used as a matrix for the composite structure. In those days, composite materials were used for basic needs like attire, sheltering, and hunting equipment for food. Despite the fact that composite materials have been used since the days of adobe, asphalt, and reinforced concrete, there was rapid development after the invention of the "condensation reaction" in the 1930s (Šerifi 2018). Composite materials have changed and improved day by day through chemistry and physics. With these improvements and the latest technology, the area of composite materials usage has expanded. Since the first applications, many innovations have been made in both reinforcement materials and matrix materials, and new composite materials with much higher performance values have been realized by applying new combinations. The industry gained tremendous momentum with the use of carbon fiber-reinforced polymer composites in the 1960s. A 60–80% weight save was possible by replacing steel with polymer fiber-reinforced composites, and a 20–50% weight save was possible by replacing aluminum. In the early days, when they were used for construction, composite materials took place in our lives to make things lighter and easier. Automobiles to defense, marine to aerospace, and biomedical industries to take care of our health composite materials were used in industries for their mechanical properties and advantages. Today, composite materials are also used as aesthetic equipment in industries like automobiles and sports.

## **1.2. Aim of thesis**

The main objective of this study is observing the filament wound cylindrical composites' mechanical and thermal properties using the finite element analysis program ANSYS. With this study, it was aimed to determine the mechanical and thermal properties by finite element method.

Another purpose is hybridizing the cylindrical structure with two different resins as matrix. In the literature, most of the hybridization studies focused on hybridizing the structure by changing the fiber type to make composite materials cheaper and more applicable to the industry. In this study, it was aimed at hybridizing the matrix material with the use of two different resins. In addition, it was desired to observe the effect of the hybridization study on the composite structure. The hybridization process was carried out during wet winding.

In this context, the following can be stated as the specific objectives of this study;

- Investigating the mechanical properties of the composite cylinders by the finite element method
- Investigating the temperature distribution of the composite cylinders by the finite element method
- Investigating the test models within the computer-aided engineering programs
- Measuring the mechanical properties and thermal conductivity values according to the standards
- Making a prediction with the failure criteria of the composite structures and verifying these results by experimental tests
- Observing the differences between the numerically simulated model and the filament wound cylindrical composite structure
- Observation of changing the resin while the cylinder is winding without curing the first resin winding. For this purpose, it is aimed to observe whether the resin change affects the deterioration of the composite structure.

### **1.3. Fundamentals of Composite Materials**

Composite materials, which are produced by combining two or more materials are divided into two parts as matrix and reinforcement materials. Matrix components are basically divided into three parts as metal matrix, polymer matrix, and ceramic matrix. The selection of matrix types is made according to the desired properties, product

geometry, and method of production. The structure of the matrix has great importance in terms of composite materials' function. The main importance of the materials that merged is to ensure thermo-mechanical stability (Balya 2004). In addition, protecting the reinforcements against environmental factors by surrounding them. Reducing and spreading the incoming impacts and making the material more durable are other important features (Balya 2004).

### **1.3.1. Metal Matrix Composites (MMC's)**

The reasons for using metal materials as matrix are their resistance to high temperatures, their strength, and no risk of burning. Moisture, which is one of the main problems in composite materials, is known to be absent in metal matrix composites (Serkan Kangal et al. 2019). The conductivity of metals is another reason to use them in composite materials. This property makes metal matrix composites useful in electrical and thermal fields. Conventional metal production processes aid the use of metal matrix composites (Serkan Kangal et al. 2019). Although, there are lots of advantages of using metal matrix composites, there are also some disadvantages. At the top of the disadvantages is being heavy of many metals. Another disadvantage is the degradation of metals' properties at the interface level. This degradation shows metal matrix composites have thermal limits (Serkan Kangal et al. 2019).

### **1.3.2. Polymer Matrix Composites (PMC's)**

Polymer matrix composites are widely used in terms of their low costs and manufacturability. This feature makes polymer matrix composites advantageous. In addition, it has been observed that these materials are stronger than steel in some polymer matrix composite samples. This sample is a graphene/epoxy composite (Serkan Kangal et al. 2019). Polymer matrix composites, which are preferred in terms of fewer costs, manufacturability, better strength, and durability, also have some disadvantages. The temperature and humidity of the area are the main factors affecting the usage of this matrix type. Being suitable for use in low temperatures and dimensional changes in humid

environments are some disadvantages of polymer matrix composites. Kevlar, glass, and graphite are the most commonly seen examples in industry (Serkan Kangal et al. 2019).

### **1.3.3. Ceramic Matrix Composites (CMC's)**

Ceramic matrix is a type that is used due to its distinctive features. The most characteristic feature is its applicability at high temperatures. This feature makes ceramic matrix usable in the heat sector. Other advantageous properties are low density and a high modulus of elasticity (Clyne and Hull 2019). These properties enable the use of ceramic matrix composites.

However, this does not mean that the ceramic matrix is without disadvantages. One of the disadvantages of ceramic matrix is its brittleness. Their non-homogeneity and low thermal and mechanical shock resistance are the features that limit their use. There are some groups of ceramics that are used for composites. These are glass ceramics, borosilicates, and aluminosilicates (Clyne and Hull 2019).

Reinforcement materials vary according to diameter, length, volume fraction, and spatial distribution. The size and alignment of additive materials change the properties of composites. Additive materials can be used as particles and fibers. In composite materials, reinforcement materials are used as particles, short fibers, long fibers, and plates. Fibers are classified according to their continuity as continuous and discontinuous fibers.

In cylindrical modeling, reinforcement materials are used as continuous fibers. Since the fibers are producing the geometry, continuous fiber types are used in cylindrical modeling. The most known fiber samples can be given as aramid, carbon, glass, and flax for cylindrical modeling (Serkan Kangal et al. 2019).

These fibers take place in the geometry as desired. The angle of the fiber changes the mechanical properties along the fiber direction. By using more than one angle, the composite material can be strengthened in more than one direction. With these improvements more reliable and cost-effective composite materials can occur. Strengthening the material with particles can be hard to disperse the additive material due to the agglomeration problem.

## 1.4. Filament Winding Technique

There are several production methods for composite materials. Usage of these methods varies according to product, dimension, and geometry (Balya 2004). Among these methods, the filament winding technique is an important one. The filament-wound product is obtained by using continuous fibers. Filament winding machines are semi-automatic machines that work on two axes. Production is made by the rotation of the mandrel and the parallel movement of the feeder to the machine. With the filament winding technique, firstly, continuous fibers come to the resin bath from the comb device. Continuous fibers get wet by resins and come to the feeding unit by getting rid of excess resin with the help of roller components. These wetted fibers cover the mandrel to generate the product. The steps of the process are shown in Figure 2. This covering of the mandrel with continuous fibers makes the product better mechanical properties (Balya 2004). Its greatest importance is its applicability on curved surfaces. The filament winding technique is applicable to cylindrical, spherical, conical, and geodesic structures (Ma et al. 2019). The filament winding method, which can be successfully applied to these geometries, is not suitable for concave shapes. It cannot be applied in concave geometries because fibers cannot touch the surface correctly. Ideal for use on axisymmetric surfaces.

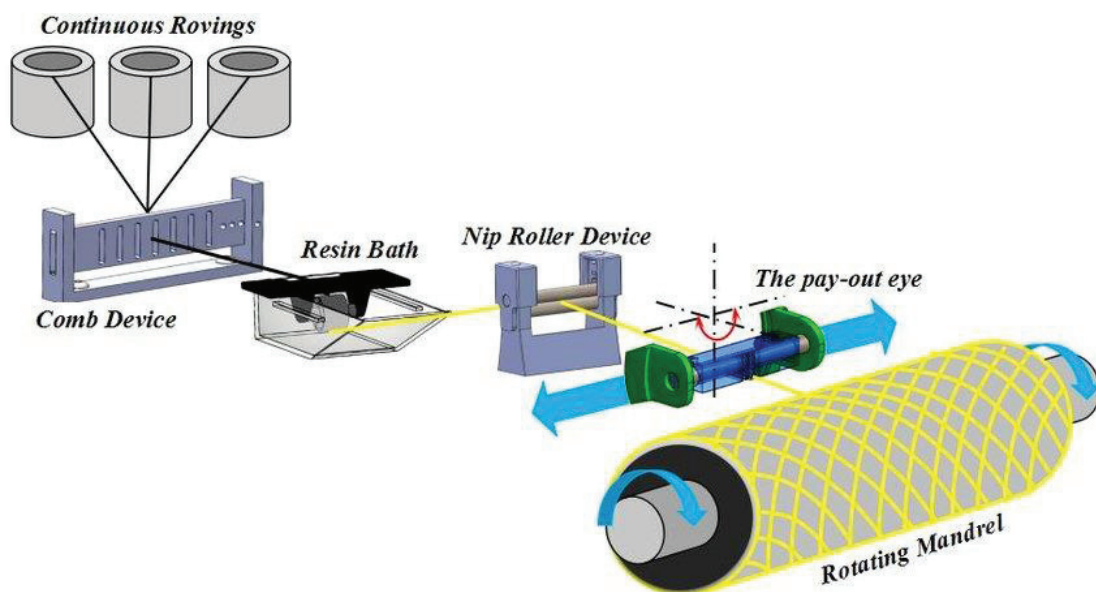


Figure 2. Filament winding technique (Source: Ma et al. 2019).

The feeding head movement speed and mandrel speed define the winding angle of the produced material. The winding turns determine the thickness of the product. For a good product, the fibers must be well packed. The tension of the fibers on the roving part is important to produce great material. This tension affects the winding process positively. There are three winding patterns in the literature. These are known as circumferential, helical, and polar (Ramkumar 2017). A circumferential pattern is a pattern in which the winding angle is approximately 90 degrees side by side with circular continuous movements. In the next round, the fibers continue to be stacked on top of each other. The helical pattern is achieved by winding the fibers at an angle along the mandrel. The winding process continues the previous laps' fibers. Polar patterning is a method generally used in spherical materials (Ramkumar 2017). In this method, the matrix material is commonly a polymer, and the most commonly used resins are thermoset resins such as epoxy. Glass, carbon, and aramid are some examples of the fibers that are used in the filament winding technique. The mandrel is quite important in this technique. Since, the mandrel specifies the geometry of the product. In filament winding technique, there are some important points about the mandrel. The mandrel must be suitable for producing a good product, easily removable and not deteriorate during curing. One of the most important parameters during the process is the tension on the fibers (Ramkumar 2017). This stress is important in terms of volume fraction and voids. The positive side of the filament winding technique is the manufacturability of products with different shapes. Another advantage is that the fibers are placed more accurately with repetition. Other advantageous features are that continuous fibers' properties are effective on the entire surface, and mandrel costs are relatively cheaper than machine tools. Even though these advantages, filament winding technique also has some disadvantages. One of the main disadvantages is, it cannot be applied to complex shapes and very small sizes. Another disadvantage is the product quality, and its mechanical properties are lower than the autoclave method (Ramkumar 2017).

## **1.5. Finite Element Method (FEM) Analysis**

Experimental processes have great importance for safety and development in engineering studies. In this context, the suitability and reliability of the designed product

are ensured by tests and experimental studies in line with the standards. However, the cost and waste of the raw materials used in these tests and experiments restrict and complicate the production. Against this situation, mathematical studies had started to work with the circular shaping of geometric model in the 1960s (Rao 2017). And it has been developed today, and the finite element method has emerged (Rao 2017). The main purpose of the finite element method is to simplify the problem (Rao 2017). When the original problem is solved by replacing it with its simplified version, the result obtained is not a precise result, it is an approximate result. In practical problems, mathematical tools will not be effective to find the exact result. It will not be effective even for an approximate result (Rao 2017).

Thus, due to the lack of suitable methods for an approximate solution, it is imperative to resort to the finite element method. The approximate result can be improved with the use of more computer systems by the finite element method to be performed (Rao 2017). This system requirement is the elements that make up the finite element method. Elements are small parts formed as a result of dividing the geometric structure into small parts. With the computational calculation of the effects on these parts, it is possible to obtain a clearer and more accurate result.

In addition to analyzing mechanical states, the finite element method is mostly used in solving many problems such as thermal conductivity, fluid dynamics, electric and magnetic fields (Rao 2017). The finite element method has been developed primarily for the aerospace sector with its use in solving different problems (Rao 2017). With this developed method, structural, thermal, electrical, and magnetic analyses can be performed.

Although it had been developed for the aerospace sector in line with the broad analysis infrastructure, it is being used in many different fields today (Rao 2017). This method is used for static analysis to predict stress, strain, and displacement of the given structure with given boundary conditions and eigenvalue analysis to observe natural frequencies, propagation situations, and the response of the structure according to the applied loads in several industries. Some of the sectors are construction, aerospace, nuclear, and biomedical engineering (Rao 2017). These sectors are using the finite element method to improve their products.

## 1.6. Thesis Outline

In the first chapter (Chapter 1), the progress starts with giving brief information about this study and explanations about headlines. The main technological topic of the thesis, composite structure, was explained as matrix and reinforcement materials, and the producing technique, filament winding was represented. After the main objective of the thesis, the finite element method (FEM) was briefly explained as applicable areas and importance of using were explained.

Chapter 2 is the literature survey part. This is the part where the studies carried out for the titles that will support this thesis are examined so far. These studies were chosen as filament winding technique, hybridization process, finite element analysis, and what are the important parameters, steps, and topics to achieve successful finite element analysis.

In Chapter 3, experimental and numerical test methods are explained in a detailed way. First, experimental test techniques and their standards were briefly given in this part. After that, for the objective finite element analysis, the steps of analysis and used parameters in this study were explained.

In Chapter 4, experimental tests and finite element analysis results were given. These results were examined by comparing the differences between experimental and finite element analysis methods. As a result of these study, filament wound composite cylinder's mechanical properties and thermal conductivity values were numerically obtained. As a result, all the obtained results were compared, and error rates are given in this part.

Chapter 5 gives a summary of the study and evaluates the parameters used. The points that provide benefits for the performed analyses are indicated, and their effects are explained. The evaluation of the values that have been realized within the framework of these effects and the possible changes that can be made are explained as a conclusion.

## CHAPTER 2

### LITERATURE SURVEY

In this chapter, filament winding technique, hybrid wound cylinder, finite element method of filament wound cylinders, and optimization of filament winding process parameters for numerical solution titles were used to get extensive information for the thesis's survey outline.

All these titles were chosen from the literature studies to prove a more apparent and systematic study. At the end of the literature survey, it was aimed to learn winding parameters according to the loads that composite cylinders encountered, how to predict the durability of the composite structure numerically and get information about test methods with these methods' criteria for finite element analysis programs.

As a result of all this research, a wide range of scanning and information acquisition from composite material information to finite element analysis information has been carried out. Since the main subject of the thesis is finite element analysis, in the literature review section, article selections were made in line with the parameters required for finite element analysis and comparison of the experimental method.

The selected studies in the literature are summarized below.

Abdallah and Braimah (Abdallah and Braimah 2022) objected to observe the mechanical performance influence of filament winding process parameters (winding angle, stacking sequence) both numerically and experimentally. For this purpose, LS-Dyna was used for the numerical solution. With this numerical work, optimal ply angle and stacking sequence values were observed. LS-Dyna is a dynamic analysis program which is added to the Ansys a few years ago.

According to the optimization study, two tube configurations were produced. These configurations are given below in Table 1. Radial compression and tensile tests are shown in Table 1.

Table 1. Specifications of produced GFRP tubes (Source: Abdallah and Braimah 2022).

Tube No.	Diameter (mm)	Total Thickness (mm)	Thickness /Layer (mm)	No. of Layers	Stacking Sequence	Type of Testing
1	155	6.4	0.4	16	[±70/±70/±70/±54/±54/±70/±70/±70]	Tension
						Radial Compression
2	155	6.4	0.64	10	[±70/±70/±54/±70/±70]	Tension
						Radial Compression

Numerical calculations were started with the mesh convergence. The results of the convergence study are given in Figure 3 as a chart.

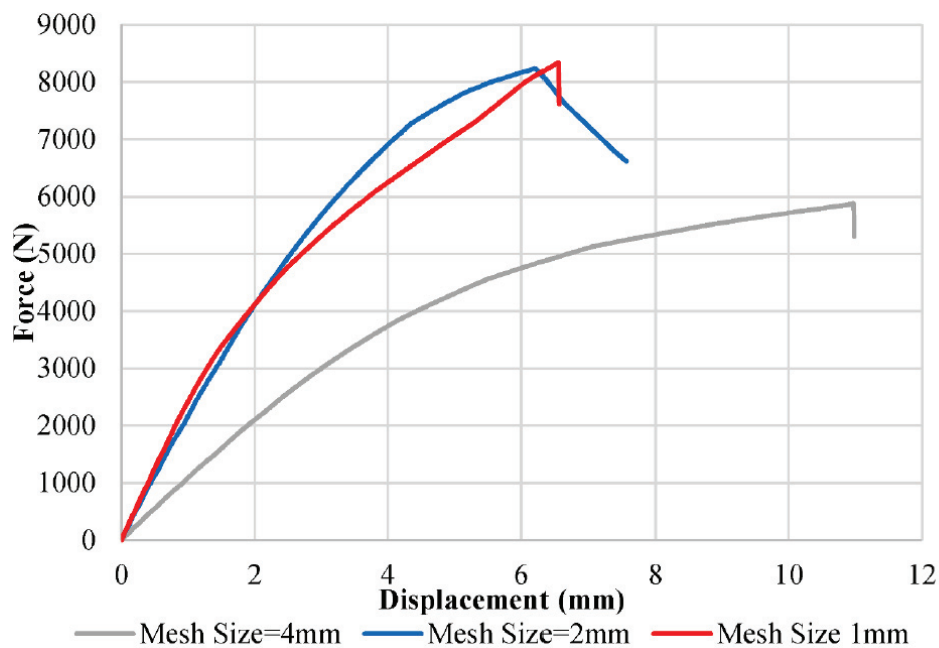


Figure 3. Comparison of the force-displacement result of mesh convergence (Source: Abdallah and Braimah 2022).

After meshing the body, tensile and radial compression tests were performed both numerically and experimentally. MAT54 type analysis system was used to predict the failure behavior of materials. These test results are given in Table 2. With this table, it was observed that the difference between experimentally and numerically analyzed test results is approximately 14%.

Table 2. Experimental results vs. numerical results for the Tube 1 and Tube 2 under radial compression test (Source: Abdallah and Braimah 2022).

Tube No	Experimental Values Maximum Load (N)	Corresponding Displacement (mm)	Numerical Values Maximum Load (N)	Corresponding Displacement (mm)	% Numerical/ Experimental	
					Load	Disp.
1	9000	7	7890	6.1	11%	12%
2	7840	8.2	7560	7.1	4%	12%

Coherent experimental and numerical solutions were observed with this study and these tests results are given as Tensile Stress-Elongation and Load-Displacement graphs in Figure 4, Figure 5, Figure 6, and Figure 7.

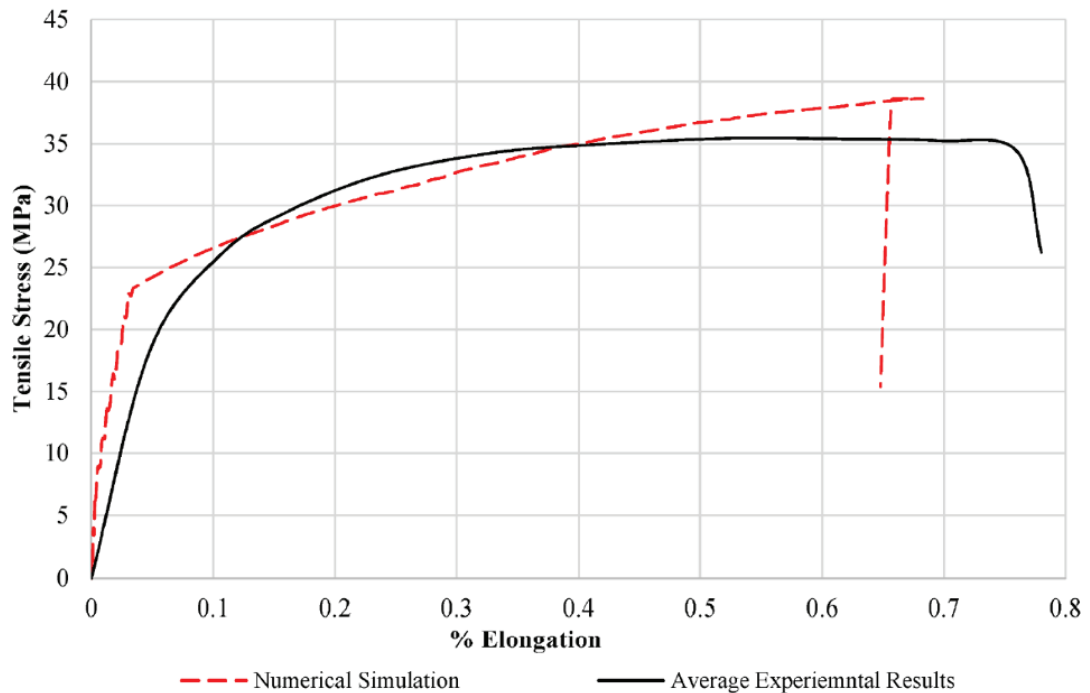


Figure 4. Tensile Stress-%elongation curves for Tube 1 (Source: Abdallah and Braimah 2022).

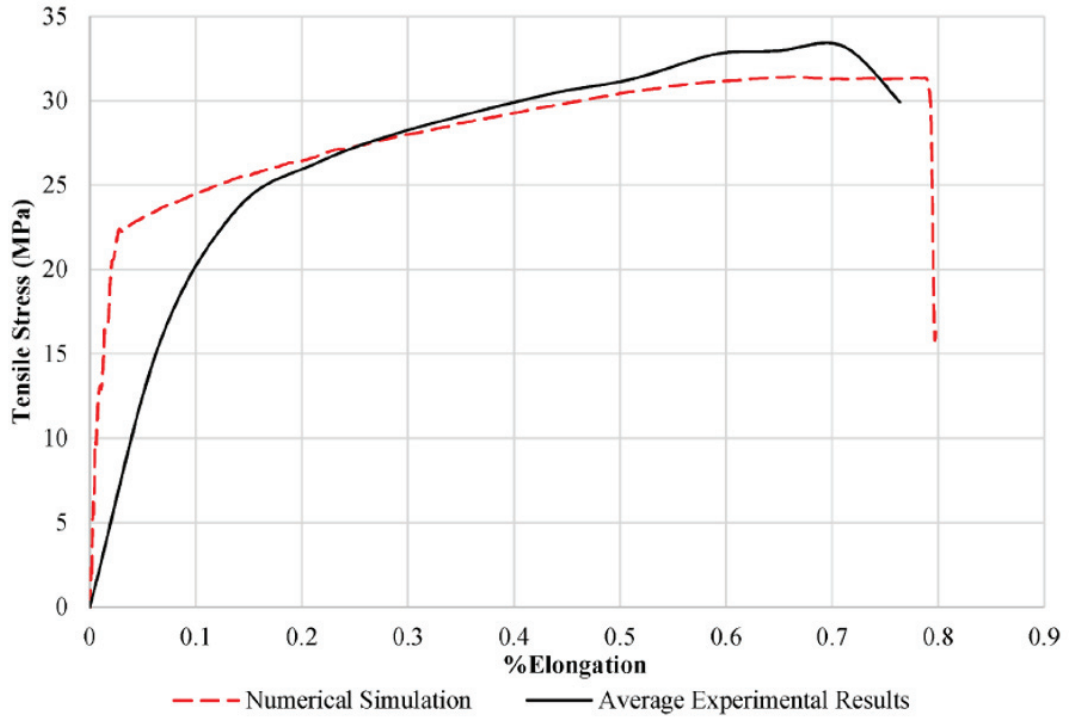


Figure 5. Tensile Stress-%elongation curves for Tube 2 (Source: Abdallah and Braimah 2022).

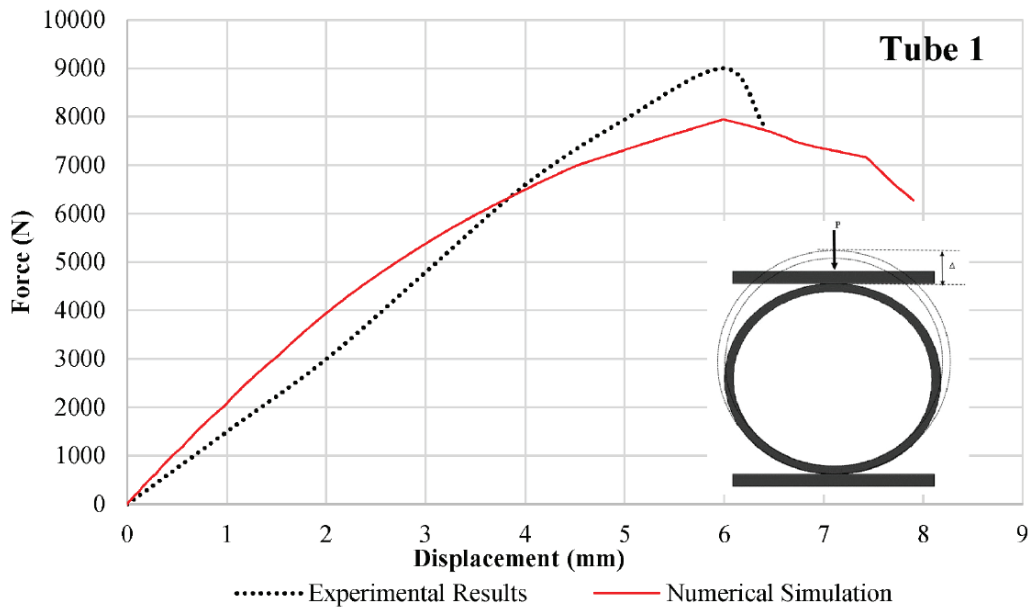


Figure 6. Load-Displacement curves for Tube 1 (Source: Abdallah and Braimah 2022).

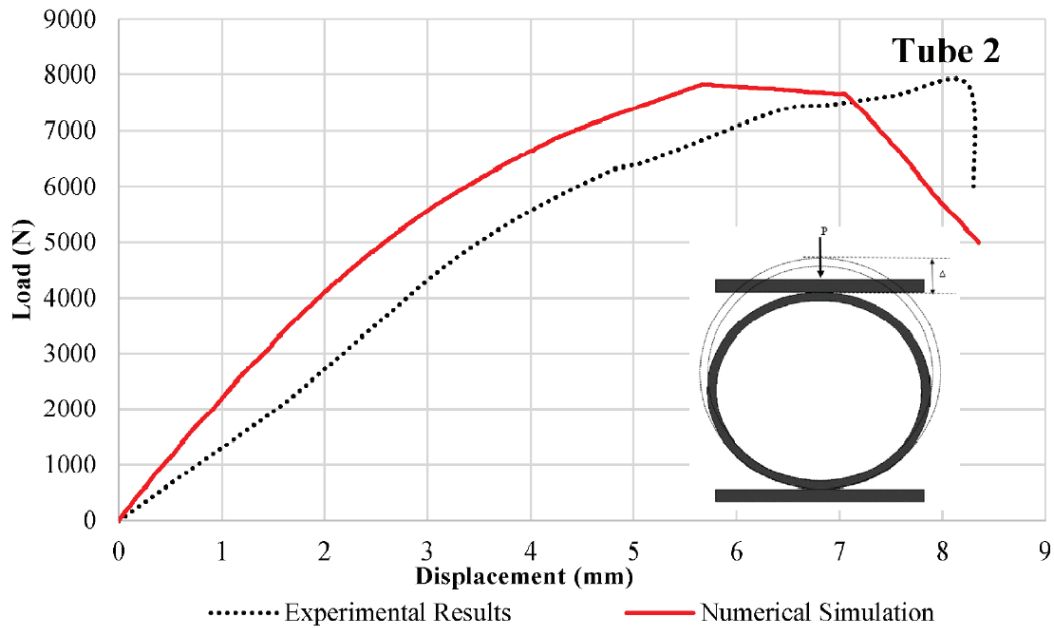


Figure 7. Load-Displacement curves for Tube 2 (Source: Abdallah and Braimah 2022).

As a conclusion of this study, it was clarified that numerical calculations are useful to predict the mechanical behavior of the composite material. Moreover, the composite layer thickness effect on the mechanical capacity was observed on a numerical simulation system, and it was revealed with two experimental specimens. While the mechanical performance was increasing with increasing layer thickness, the construction time and cost were increasing. The importance of the configuration of the composite material was validated with these experiments. The boundary condition and load directions determine the winding angle. If better tensile strength is desired, the winding angle should be close to the force direction. The tensile condition showed the failure in the narrow-gauge section. By the time radial compression tests were examined, the main failure mode occurred in the delamination regions.

Arslan et al. (Arslan Özgen et al., 2019) examined a well-known car part drive shaft. This study's objective material is a composite drive shaft to reduce some of the pros of a metal drive shaft. Firstly, a metal drive shaft is produced in two parts. This situation is designed to increase fundamental bending and natural frequency to make products safer. The Novelty of the study is reducing the pieces to one. And producing this piece from composite materials with hybrid stacking sequence configurations. To achieve this purpose, carbon/epoxy and glass/epoxy composite materials were used. With these two types of composites, it was wanted to optimize cost/performance status. To predict the

conditions and save the waste material, numerical modeling was previously used. The configuration of the composite structures is given in Table 3. The boundary conditions are given in Figure 8.

Table 3. Stacking sequence of specimens (Source: Arslan Özgen et al. 2019).

Specimen ID	Stacking (Inward)	D <sub>in</sub>   D <sub>out</sub> (mm)
82.1Cb15(55)	C[±55] <sub>15</sub>	70   82
82.6CII10(55)	G[±55] <sub>10</sub>	70   82.6
80.2Cb6GI6(55)	C[±55] <sub>6</sub> +G[±55] <sub>6</sub> t <sub>c</sub> =2.75 + t <sub>g</sub> =2.55	70   80.6
82.8GI6Cb6(55)	G[±55] <sub>6</sub> +C[±55] <sub>6</sub> t <sub>g</sub> =3.3 + t <sub>c</sub> =3.1	70   82.8
81.2GI4Cb8(55)	G[±55] <sub>4</sub> +C[±55] <sub>8</sub> t <sub>g</sub> =2.2 + t <sub>c</sub> =3.4	70   81.2
80Cb8GI4(55)	C[±55] <sub>8</sub> +G[±55] <sub>4</sub> t <sub>c</sub> =3.35 + t <sub>g</sub> =1.65	70   80

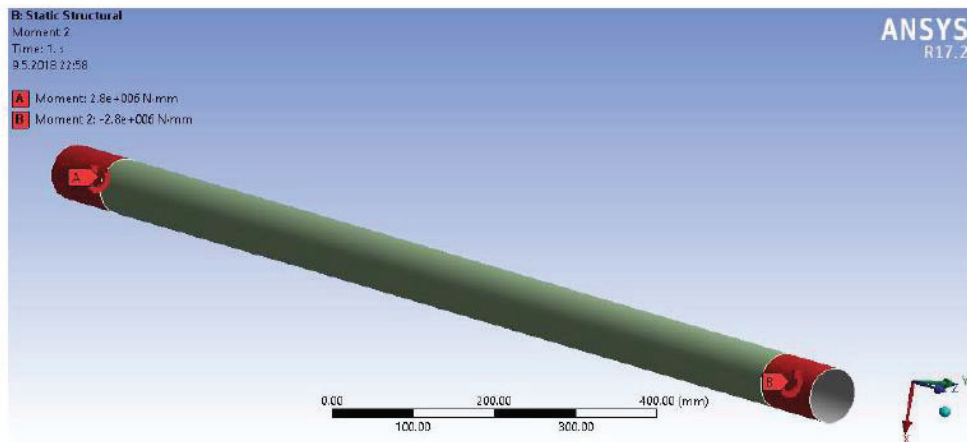


Figure 8. Moment application at both ends through insert contact surfaces (Source: Arslan Özgen et al. 2019).

Anslys library data was used to observe failure criteria. The result of these observations, FEM torque capacity, and critical buckling torque resultant values are given in Table 4. and the eigenvalue buckling analysis picture is given in Figure 9.

As a result of this study, the maximum error was observed as 14%. Other noted part is volume fraction importance. For the more coherent results between experimental and finite element analysis, it is more beneficial to get mechanical properties from the wound product.

Table 4. FEM results for the torsional capacity and critical buckling torque of the specimens (Source: Arslan Özgen et al. 2019).

Specimen ID	FEM torque capacity (Nm)	FEM critical buckling torque (Nm)
82.1Cb15(55)	2600	28600
82.6CI110(55)	1440	16450
80.2Cb6GI6(55)	2000	19000
82.8GI6Cb6(55)	3000	26500
81.2GI4Cb8(55)	2880	18000
80Cb8GI4(55)	1640	15260

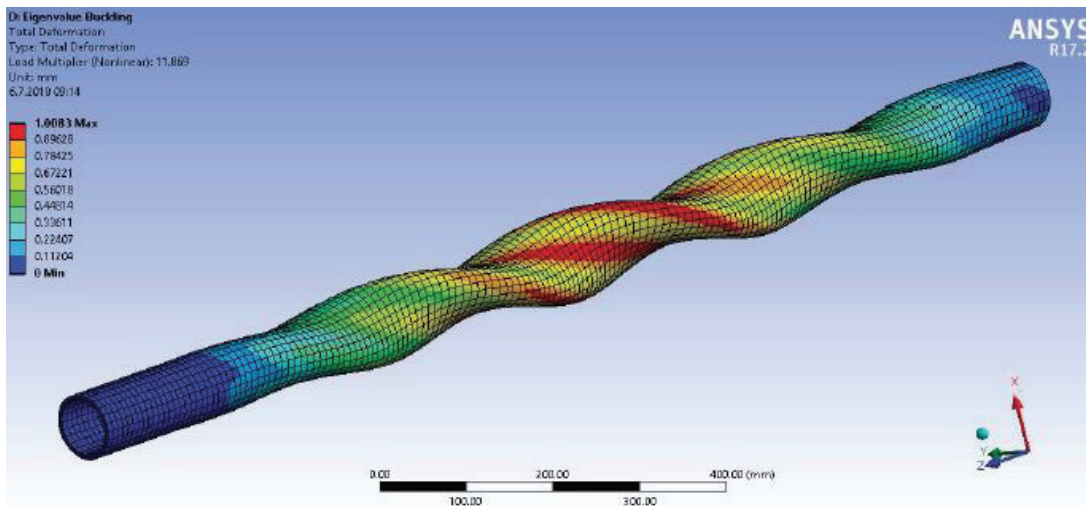


Figure 9. Torsional buckling analysis typical torsional buckling mode (Source: Arslan Özgen et al. 2019).

Toh et al. (Toh et al. 2018) were tried to characterize the main objective material composite pipes correctly. While it is possible to predict flat-wise properties with lamina theory, lamina theory is not applicable for cylindrical composites. Experimental studies started with estimating materials' properties. These properties were obtained from UD-formed composite materials, and these values were used in the prediction of angle using the procedure. In the literature, they showed uncertainty from other same-step studies. This situation was noted because of fiber and matrix differences and the composite structure's volume fraction differences. For more suitable and coherent output data, one flowchart was used in this study. This flowchart is given in Figure 10.

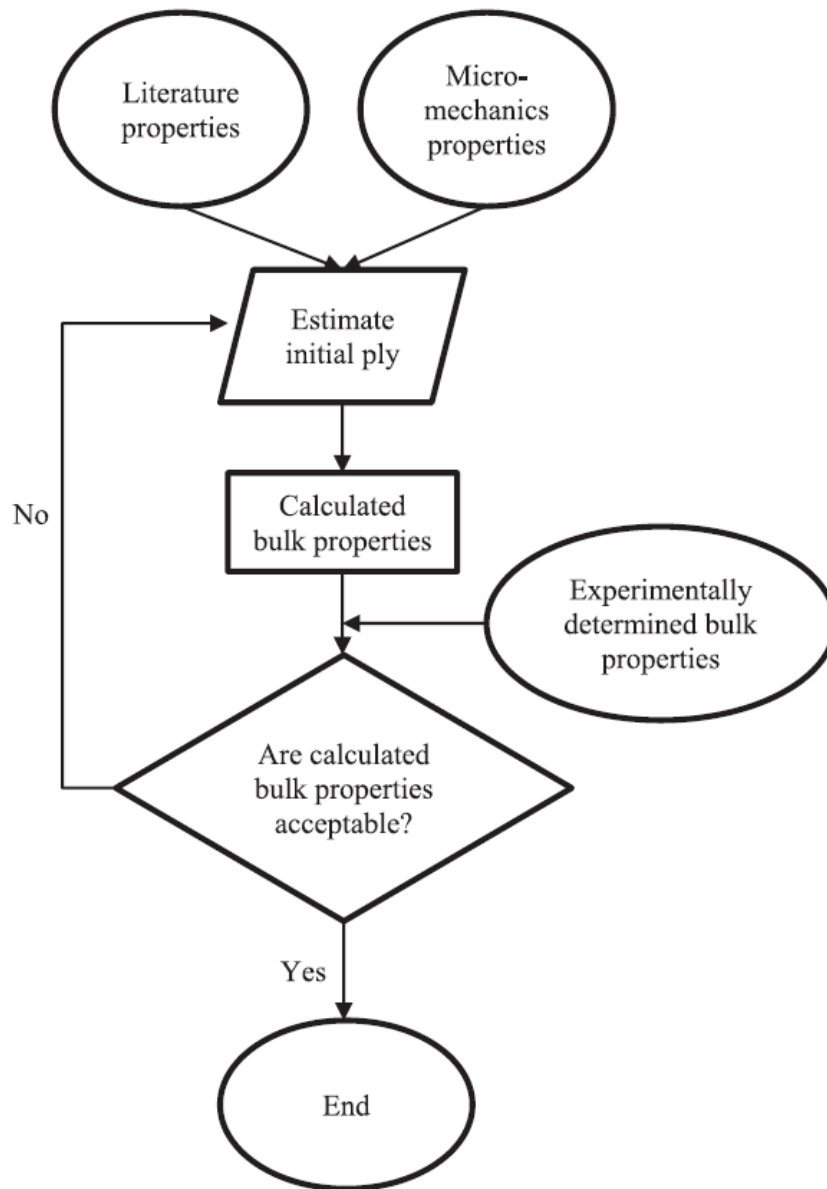


Figure 10. Flowchart for iteration of suitable ply properties (Source: Toh et al. 2018).

After getting the material properties, a determination of pipe properties study was started. This study performed some tests according to standards. Applied test methods and standards are given in Table 5. For prediction and gain time, numerical calculations were performed in the finite element analysis program ABAQUS. The modeled figures are given in Figure 11.

Table 5. Test matrix and correspond standards (Source: Toh et al. 2018).

Test	Test Standards	Specimen Section
Uniaxial tensile	D3039/D3036M-95	(a)
Uniaxial compression	D6641/D6641M-09	(b)
Ring stiffness	BS EN 1228:1997	(c)
Circumferential tensile	BS EN 1394:1997	(d)

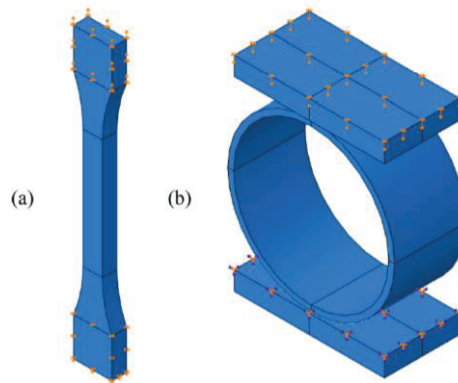


Figure 11. Finite element models for the (a) uniaxial tensile test and (b) ring stiffness test (Source: Toh et al. 2018).

As a conclusion of this study, the axial and circumfixal properties of glass/epoxy composite pipe were observed. A successful derivation was performed for ply-level properties according to stress homogenization theory. Then, interactional theory estimates properties that are obtained from both literature and micromechanics studies. The performed finite element modeling study showed consistent results with experimental studies' results. Moreover, the finite element method found successive predictions of composite failure mechanisms and stress distribution ply by ply. Numerical and experimental force-displacement curves are given in Figure 12.

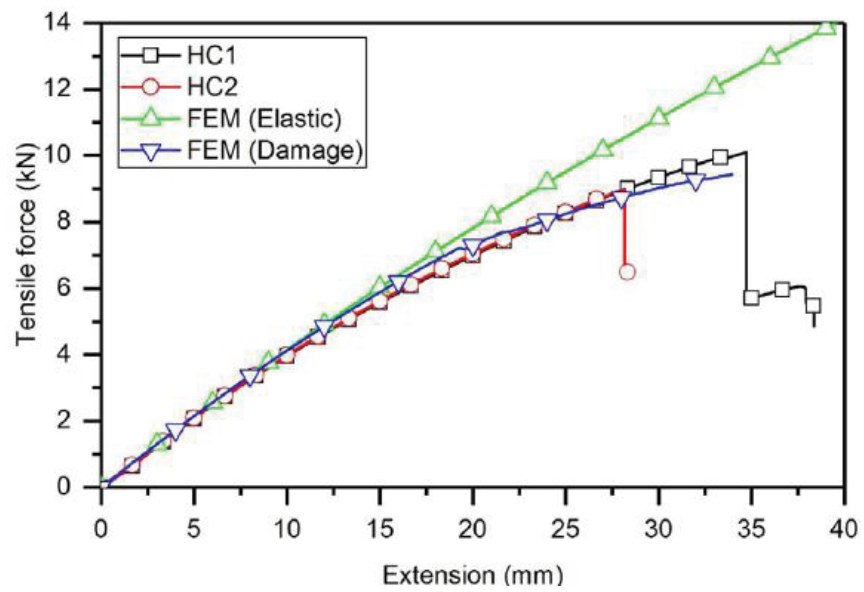
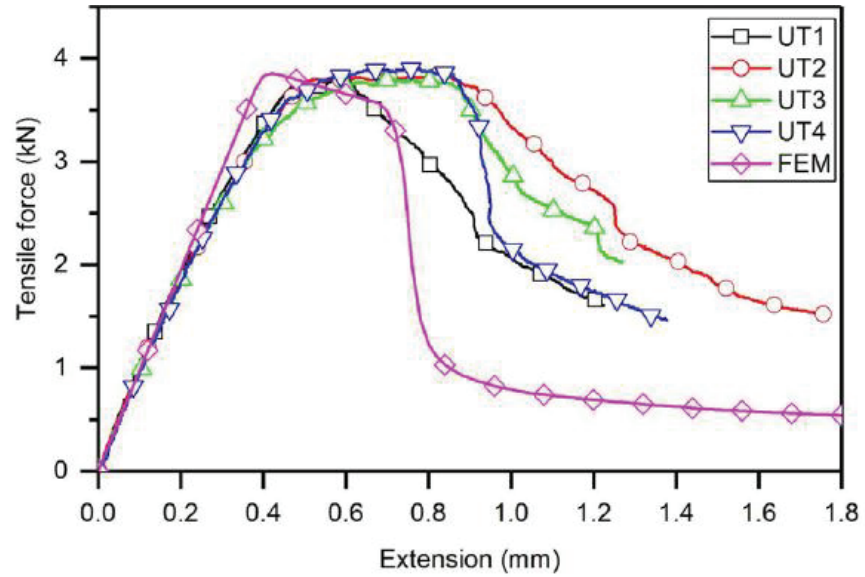


Figure 12. Force-displacement curve of the (a) uniaxial tensile test and (b) ring stiffness test (Source: Toh et al. 2018).

Gunasegaran et al. (Gunasegaran, Prashanth, and Narayanan 2013) was aimed to make an investigation of glass fiber reinforced plastic pipes according to four process parameters. For experimental procedure, test samples were produced by Taguchi's design of experimental model. With this model, study was optimized by axial tensile strength, hoop tensile strength and pipe stiffness. Determining the weight of every single part was examined statistically with ANOVA method. To realize the scenario of conditions that pipes encounter, finite element analysis was performed.

All in all, in these works, it was tried to optimize glass fiber reinforced plastic pipe. In parametric optimization, parameters were chosen in two titles. The first parameter title is "process control parameters," and there are four process control parameters.

The second title is "mechanical properties as response variables." These parameters are given in Table 6. In Taguchi's method, experiments found appropriate orthogonal arrays. These foundations are given in Tables 7 and 8.

Table 6. List of variables (Source: Gunasegaran et al., 2013).

Control variables				Response variables		
Winding angle (A)	Silica content by weight (B)	Silica particle size (C)	Fiber pretension (D)	Axial tensile strength	Hoop tensile strength	Pipe stiffness

Table 7. L9 orthogonal array(Source: Gunasegaran, Prashanth, and Narayanan 2013).

Experiment	Levels of control variable			
	Winding angle (A)	Silica content by weight (B)	Silica particle size (C)	Fiber pretension (D)
1	1	1	1	1
2	1	2	2	2
3	1	3	3	3
4	2	1	2	3
5	2	2	3	1
6	2	3	1	2
7	3	1	3	2
8	3	2	1	3
9	3	3	2	1

Table 8. Magnitudes of control variables (Source: Gunasegaran, Prashanth, and Narayanan 2013).

Control variable	Level		
	1	2	3
Winding angle (degree) (A)	55	63	73
Silica content by weight (%) (B)	20	30	40
Silica particle size (microns) (C)	300	500	700
Fiber pretension (gms/roving) (D)	100	125	150

Test results were obtained by Universal Testing Machine (UTM). Obtained tests are axial tensile strength according to the ASTM D638 standard, hoop tensile strength according to the ASTM D2290 standard, and pipe stiffness according to the ASTM D2412 standard. These test data were analyzed by using Taguchi Result Model and using ANOVA.

To confirm analysis with experiments, optimized axial tensile strength, hoop tensile strength, and pipe stiffness were found as 40.10 MPa, 301,24 MPa and 558,05 kPa respectively. In the finite element analysis, the composite pipe was modeled as a linear SHELL99 element. Boundary conditions were given as internal pressure of 6 bars, external load due to soil overburden to a minimum cover depth of 1,5 m, and pipe constrained in the vertical direction alone at the bottom of the pipe. As similar as the experimental test procedures defined with this numerical solution system. The damage propagation og the composite cylinders and stress distribution was observed in this article.

To conclude of study, optimum combinations were achieved for these three test methods. These results are obtained by given ASTM standards.

Optimized configurations are:

For Axial Tensile Strength, optimum combination was found as A1 B1 C1 D3.

For Hoop Tensile Strength, optimum combination was found as A3 B1 C1 D1.

For Pipe Stiffness, optimum combination was found as A2 B3 C1 D3.

Nodal solutions of these optimized combinations pictures are given in Figure 13 and the values of optimal designs are given in Table 9.

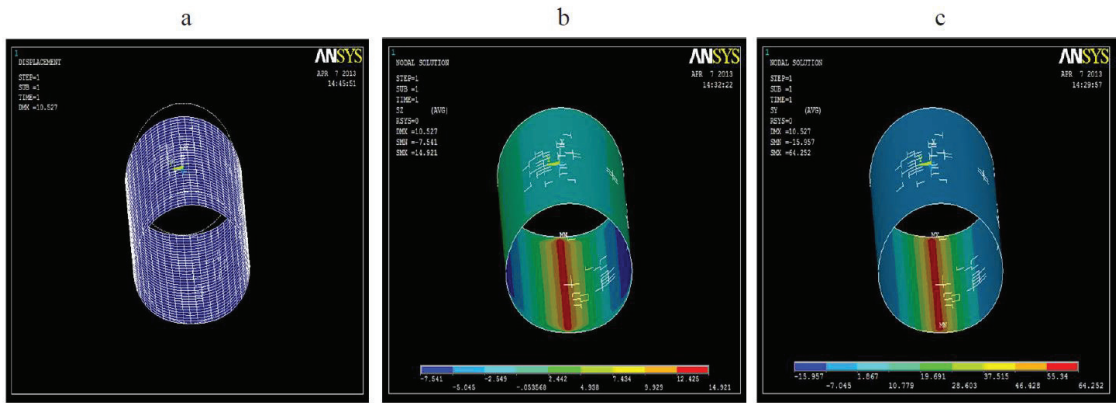


Figure 13. (a) Plot for hoop deformation; (b) Plot for axial stress; (c) Plot for hoop stress (Source: Gunasegaran, Prashanth, and Narayanan 2013).

Table 9. Nodal solutions for optimized pipes (Source: Gunasegaran, Prashanth, and Narayanan 2013).

Optimum setting	Maximum axial stress (Mpa)	Maximum hoop stress (Mpa)	Maximum hoop deflection (mm)
A1 B1 C1 D3	14.921	64.252	10.527
A3 B1 C1 D1	14.479	62.809	15.974
A2 B3 C1 D3	14.728	63.780	10.404

Maziz et al. (Maziz et al. 2021) was performed using a hybridized cylindrical composite as fiber material. Pressurized hybrid composite pipes were produced by the filament winding process. The desired system in this study was programmed as a 3D FE model to predict impact loads and damage formation for pressurized hybrid composite pipes in the finite element modeling program ABAQUS.

A 3D finite element model was used to establish damage models for intralaminar and interlaminar scale damage. Hashin failure criteria were used for predicting intralaminar damage. For interlaminar damage, cohesive zone elements were used to evaluate failure. It was expected that there would be compatible resultant data between the modeling result and the experimental result.

The damage model steps that had been programmed in ABAQUS are shown in Figure 14.

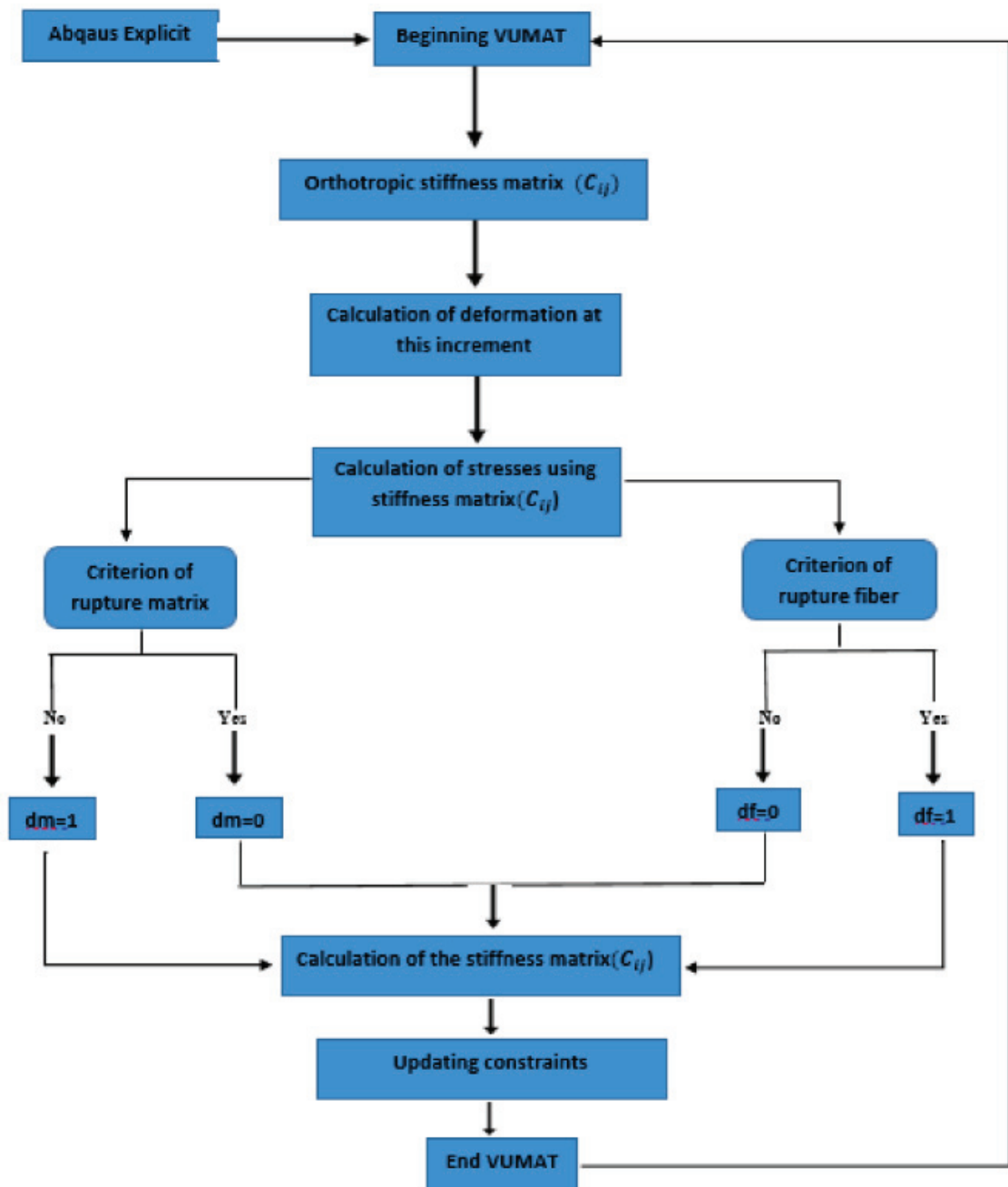


Figure 14. Numerical damage modelling in Abaqus (Source: Maziz et al. 2021).

In this extensive research, the given pipe geometry and analyses' boundary conditions are shown in Table 10 and Figure 15, respectively. With this geometry, low-velocity impact tests were applied between 5 and 20 J energy levels while the pipe had a 32-bar internal pressure.

Table 10. Geometry of the hybrid pipe (Source: Maziz et al. 2021).

Internal radius, $R_i$ (mm)	External radius, $R_e$ (mm)	Tube Length, $L$ (mm)	Stacking sequence
36	38.4	300	$[\pm 55]_3$

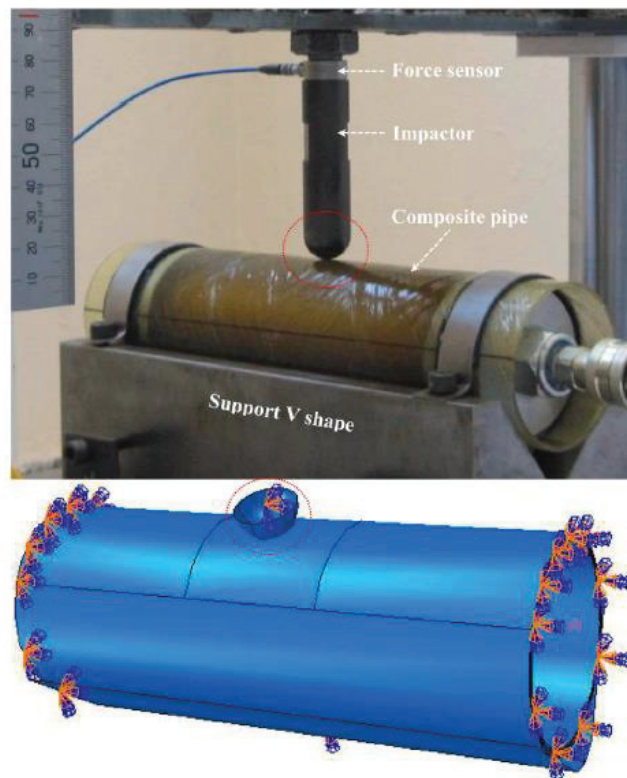


Figure 15. Boundary conditions of hybrid composite pipe (Source: Maziz et al. 2021).

In this paper, it was tried to find out the main defects in composites under impact loading. And it was observed to find a solution with the hybridization process. This hybridization process was investigated by changing the stacking sequence of composite pipes. These configurations are given in Figure 16.

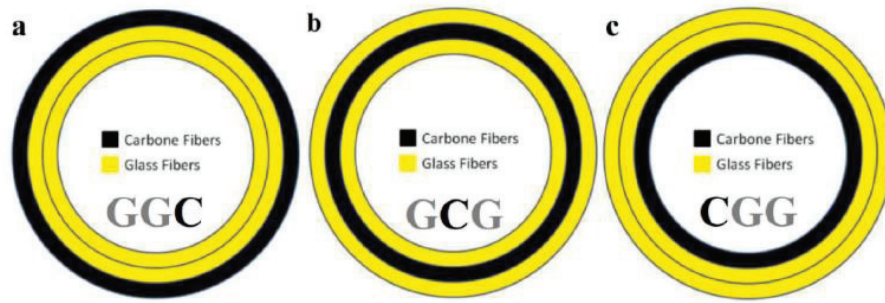


Figure 16. Composite materials and stacking sequence (Source: Maziz et al. 2021).

As a result of this study, numerically modeled pressurized composite pipes have been examined. This model showed the ability to predict the impact scenarios before the experimental testing of pipes. Moreover, different models, according to their stacking sequences, were validated with experimental processes. As a conclusion of this paper, the described delamination performance of hybrid composite pipes with different stacking sequences is shown in Figure 17.

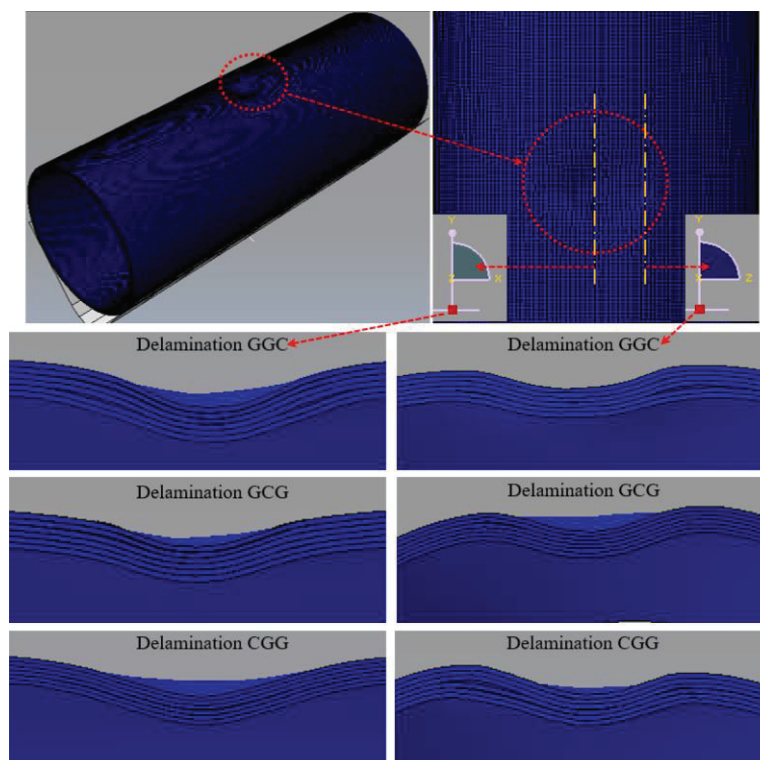


Figure 17. Predicted delamination according to the different stacking sequences through the thickness (Source: Maziz et al. 2021).

Zacharakis et al. (Zacharakis et al. 2022) was expected to find the lamina's mechanical properties of filament wound pipe and optimize the structure using finite element analysis, validating this analysis by experimental linear and non-linear characteristics.

For this purpose, the homogenization method was first used to obtain the nominal values of layer properties. The second step was a simple tensile test according to ASTM standards.

Finally, in this work, tensile-based validation tests were applied according to the materials and process parameters. Finding the parameters in filament-wound pipe is hard because of the complex structure of the composite material.

This hard condition was solved by following some steps to find the optimal parameters. These steps are shown in Figure 18 as a flow chart. Pre-information was obtained with tensile tests. Test configurations are given in Table 11.

After the extensive work, found parameters and mechanical parameters were used in the finite element analysis program Nastran. To validate all these results, three test procedures were examined in Nastran. These tests are three-point bending, the ring (hoop tensile) test, and radial deformation.

Table 11. Tensile Test Specifications (Source: Zacharakis et al. 2022).

<b>Specimen Properties</b>	
<b>Layer orientation</b>	$(+/-55) / (+/-55)$ $/ (+85) / (+/-55) /$ $(+/-55)/(+/-55)$
<b>Layer Thickness</b>	$+/-55 \rightarrow 0.35$ $85 \rightarrow 0.16$
<b>Tube Internal Diameter</b>	220 mm
<b>Free Height</b>	122 mm
<b>Width</b>	22 mm

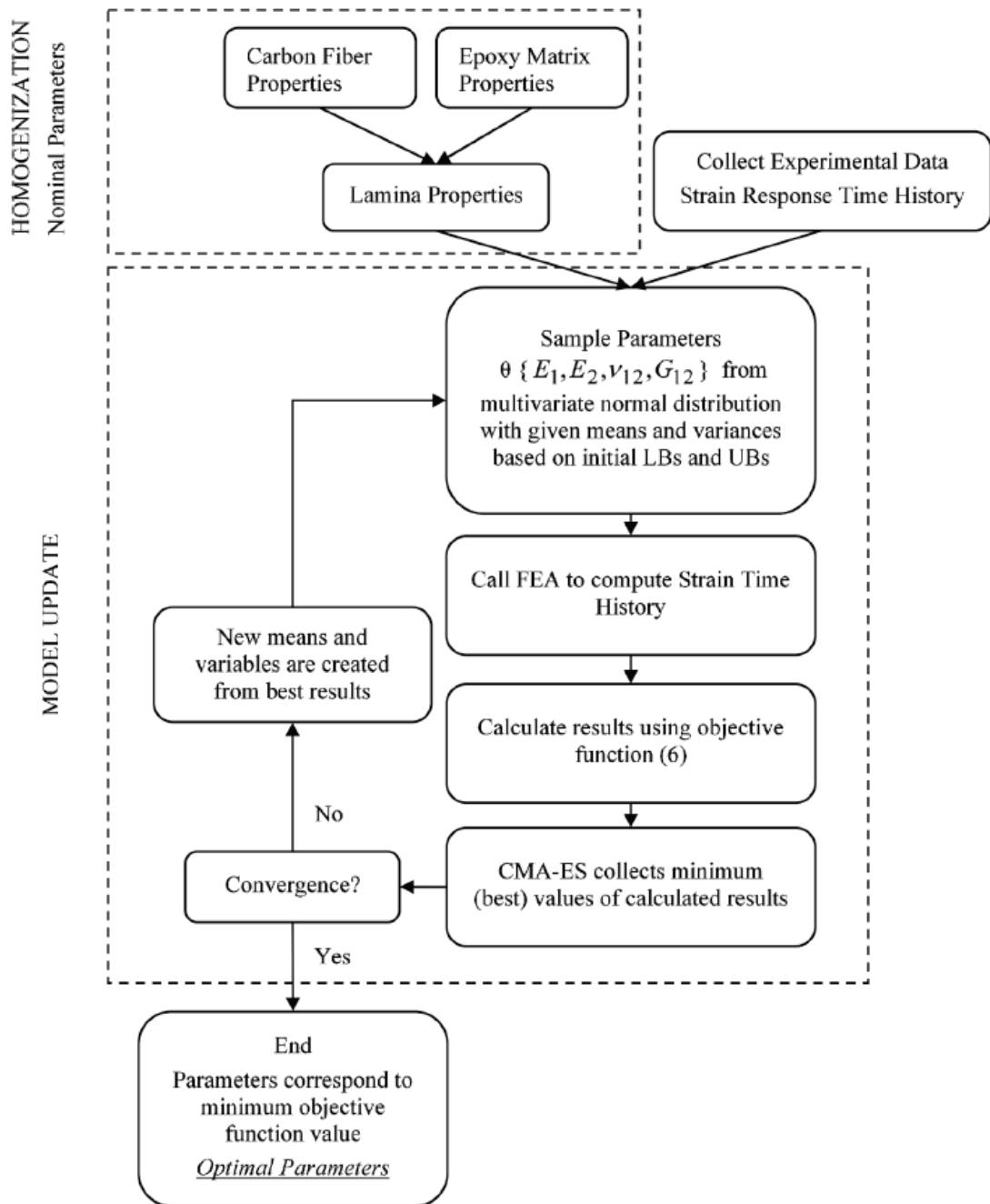


Figure 18. Applied steps to find optimal parameters flow chart (Source: Zacharakis et al. 2022).

Three-point bending and ring test layout, analysis modeling, and test photos, both experimental and numerical, were given in Figures 19 and 20, respectively.

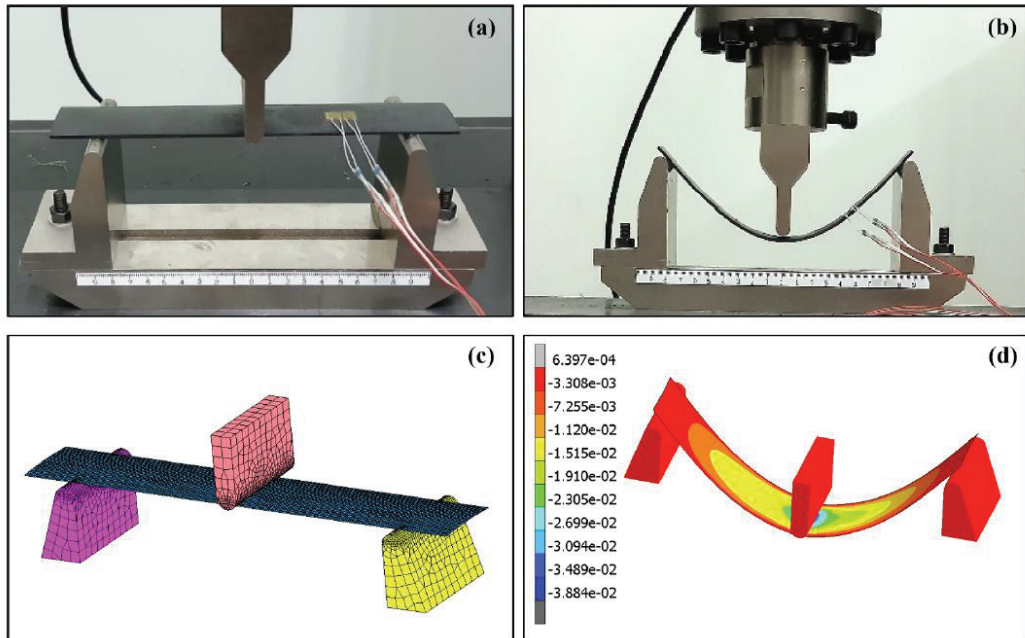


Figure 19. Three-point bending pictures. (a) experimental model, (b) experimental maximum bending, (c) numerical model, (d) numerical maximum bending (Source: Zacharakis et al. 2022).

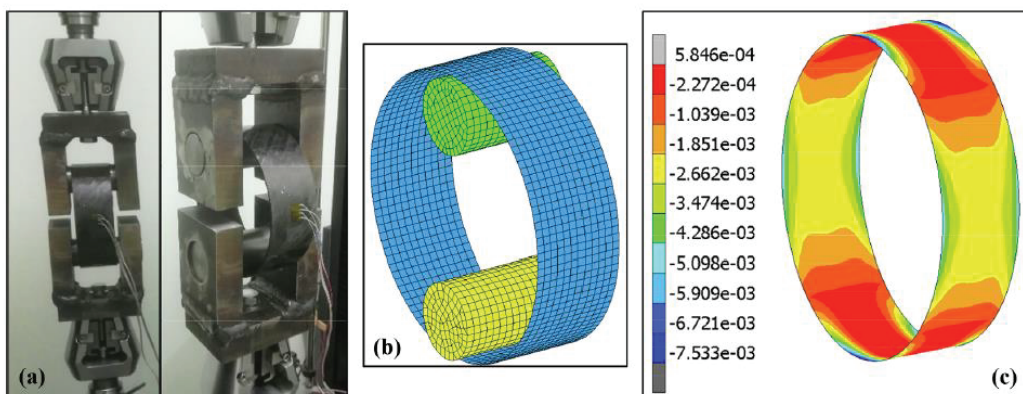


Figure 20. Ring test layout. (a) experimental model, (b) numerical model, (c) numerical test result (Source: Zacharakis et al. 2022).

As a conclusion of the study, an optimally modeled process was found and validated with extensive effort. These efforts provided evidence of the effectiveness of this methodology. Moreover, it showed the effectiveness of finite element modeling to predict the damage path and failure. These predictions help to improve the material according to the conditions that it encounters at a lower cost.

## **CHAPTER 3**

### **METHODOLOGY**

To clarify the investigation of composite materials' mechanical and numerical analysis results, there are some methodologies that must be employed, respectively. The material properties of the composite structure that were analyzed numerically are vital to predicting more precise results. For this purpose, composite materials' mechanical properties were found by experimental procedures. With these values, more accurate analysis results were expected to be obtained from numerical analysis. The more appropriate the material data, the greater the chance to improve the system.

#### **3.1. Experimental**

Experimental processes are explained with materials information as fiber and matrix material. Then, experimental tests and used standards of these tests are illustrated.

##### **3.1.1. Materials**

The technical information, names, and usage patterns of all materials used are explained in this section.

###### **3.1.1.1. Fiber**

In this study, DOWAKSA 12K A-49 continuous carbon fiber reinforcement filament was used to create composite structure. The carbon fiber's properties that are used in this research are given in the Table 12.

Table 12. The properties of DOWAKSA 12K A-49 continuous carbon fiber from data sheet.

	English		Metric		Test Method
Tensile Strength	710	ksi	4900	MPa	ISO 10618
Tensile Modulus	34.8	Msi	240	GPa	ISO 10618
Strain	2	%	2	%	ISO 10618
Density	0.065	lbs/in <sup>3</sup>	1.79	g/cm <sup>3</sup>	ISO 10619
Yield	1.862	ft/lbs	800	g/1000m	ISO 1889
Sizing Type & Amount	D012		1.0-1.5	%	Iso 10548
Twist	Never twisted				

### 3.1.1.2. Resin

Two types of resins were used in this study as epoxy and phenolic. The used Epoxy resin system is Araldite Impregnating Resin System that occurs by Araldite MY 740 Resin, Aradur HY 906 Hardener and DY 070 Accelerator. As a Phenolic Resin FX-300 model resin was used from “EPAKEM KİMYA”. Product data of these materials are given in the Table 13.

Table 13. Fiber and resins viscosity and density properties.

	Araldite MY 740 Epoxy Resin	Fenolinn FX-300 Phenolic Resin	Aradur HY 906 Hardener	DY 070 Accelerator
Viscosity	10000-14500 mPa·s	12000-15000 mPa·s	175-300 mPa·s	<50 mPa·s
Density	1.15-1.20 g/cm <sup>3</sup>	1.10 g/cm <sup>3</sup>	1.20-1.25 g/cm <sup>3</sup>	0.95-1.05 g/cm <sup>3</sup>

### 3.1.2. Composite Structure Production

Composite structures were produced with Fibermak Composites Inc. The CNC-controlled filament winding machine according to the geometries of the desired purposes. This machine has 4 degree of freedom capacity to produce cylindrical structures.

### 3.1.2.1. Composite Plate

The purpose of producing composite plates is to be used in some analyses to observe certain values for finite element analysis material needs. These plates were produced with a CNC-controlled filament winding machine with a nearly 90-degree winding angle. Hoop winding was used to obtain the composite material's UD mechanical properties. Acquired values of composite plates are used as a reference for the analysis material data as UD 0-degree composite structure. The explained composite plate production process is given in Figure 21.

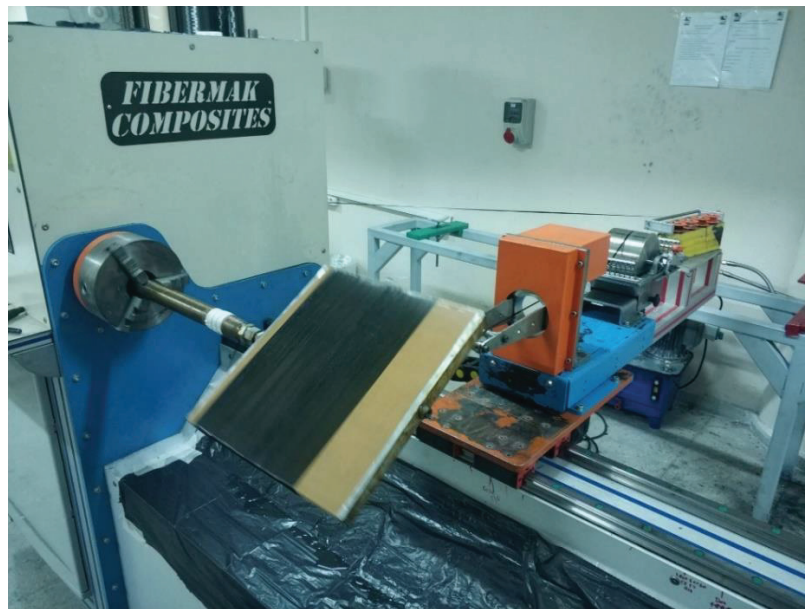


Figure 21. A view of producing operation of composite plate.

### 3.1.2.2. Composite Cylinder

Composite cylinders were manufactured to obtaining the test materials parts according to the expected dimensions. All these test specimens are obtained by producing composite cylinders. 55-degree winding angle was used as a winding angle.

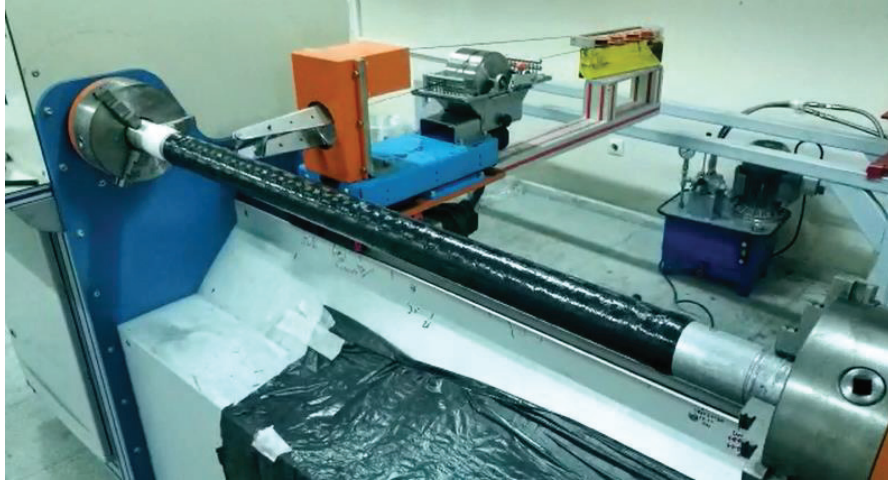


Figure 22. A view of winding operation of composite cylinder.

### **3.1.3. Test Methods**

In this part, the produced materials are tested under two conditions. The first condition is plate testing. These tests were performed to achieve material properties for the finite element method. The second condition is cylindrical testing. The objectives of the composite cylinder tests are a comparison of the numerical results to the experimental results.

#### **3.1.3.1. Plate Tests**

To obtain the composite structures' mechanical and thermal properties, some processes were followed. Getting the required material data, "Tensile Test," "Combine Loading Test," "V-notch Beam," and "Thermal Conductivity" tests were performed.

##### **3.1.3.1.1. Tensile Test**

The specimens were subjected to controlled stress to failure using a Shimadzu AGS-X universal testing machine at a crosshead speed of 2 mm/min. The tensile tests were carried out on at least three specimens, and the values for tensile strength, modulus

of elasticity, and deformation at break were calculated. The standard procedure, ASTM D3039, for tensile testing was followed.

$$\sigma_i = \frac{P_i}{A} \quad (3.1)$$

A test specimen is shown in the Figure 23.

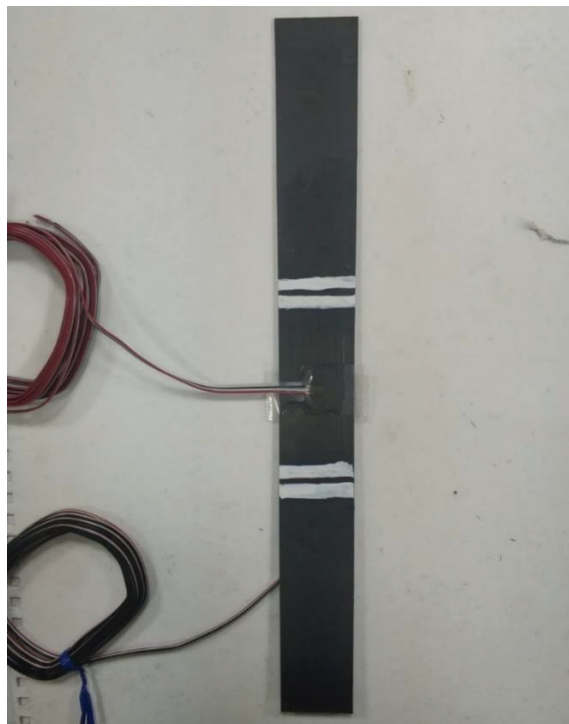


Figure 23. A view of test specimen.

### **3.1.3.1.2. Combine Loading Test**

The test specimens were tested by a Shimadzu AGS-X universal testing machine to actualize combined end- and sear loading to obtain composite materials' compressive strength and stiffness properties. In the combined loading test, the standard dimensional requirement and amount of specimen have been chosen according to the ASTM D6641 standard. Test specimens are given in Figure 24.

$$F^{CU} = \frac{P_f}{wh} \quad (3.2)$$

Where,  $F^{CU}$  is laminate compressive strength,  $P_f$  is maximum load to failure,  $w$  is specimen gage width and  $h$  is specimen gage thickness.



Figure 24. The Combined Loading Test Specimens.

### 3.1.3.1.3. V-Notch Beam Method

In the V-Notched Beam Method, notch specimens are loaded along the fiber or perpendicular to the fiber to obtain composite materials' shear properties. These specimens are prepared to be tested with V-shaped notches at the middle part of the test materials, which have a  $45^\circ$  angle to the normal of the specimen, and two orthogonal strain gauges.

This method was carried out following the ASTM D 5379 standard on the Shimadzu Universal Testing Machine. After the product size and the test sample were

produced under appropriate conditions in accordance with the standards used, the results were obtained from the testing of three test samples with similar dimensional properties.

One of the test specimens is given in Figure 25.

$$F^u = P^u / A \quad (3.3)$$

$$\tau_i = P_i / A \quad (3.4)$$

where,

$F^u$  = Ultimate strength, MPa [psi]

$P^u$  = The lower of ultimate or load at 5% shear strain, N [lbf]

$\tau_i$  = Shear stress  $i^{\text{th}}$  data point, MPa [psi]

$P_i$  = Load at  $i^{\text{th}}$  data point, N [lbf]

$A$  = Cross-sectional area,  $\text{mm}^2$  [ $\text{in}^2$ ]

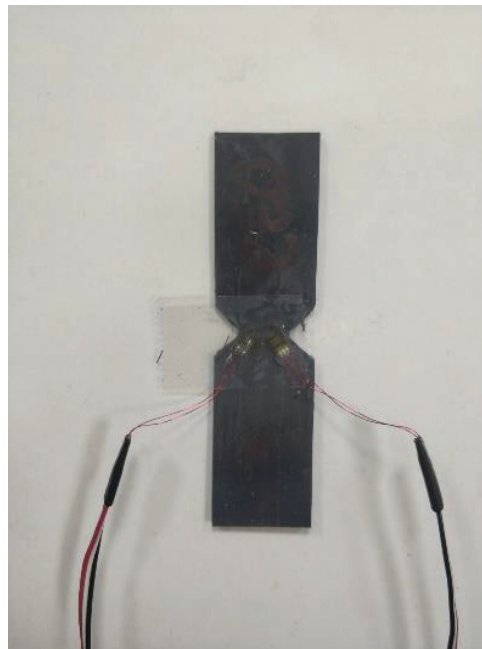


Figure 25. A view of V-Notch Beam test specimen.

#### **3.1.3.1.4. Thermal Conductivity**

Thermal conductivity meter KEM QTM 500 was utilized to observe thermal conductivity values of polymer matrix composite materials. With thermal conductivity measurement it was objected to achieve heat transmission coefficients of the produced composite materials. KEM QTM 500 machine was shown in Figure 26.



Figure 26. KEM QTM 500 Thermal conductivity meter.

#### **3.1.3.2. Composite Cylinder Tests**

Produced composite cylinders were tested to observe expected material properties. These steps are explained in a detailed way.

##### **3.1.3.2.1. Three Point Bending**

Three-point bending tests are used to predict the flexural properties of polymer matrix composite materials. According to the ASTM D7264 standard flexural stiffness

and strength properties of specimens were obtained by Shimadzu™ AGS-X universal testing machine.

Procedure A was used in the ASTM D7264 standard which has three-point loading system that illustrate center loading on a simply supported beam. The test setup was given in Figure 27.

Maximum flexural stiffness is represented with following equation:

$$\sigma = \frac{3PL}{2bh^3} \quad (3.5)$$

where,

$\sigma$  = stress at the outer surface at mid-span, MPa [psi],

P = applied force, N [lbf],

L = support span, mm [in.],

b = width of beam, mm [in.], and

h = thickness of beam, mm [in.].



Figure 27. Three-point bending test setup.

### 3.1.3.2.2. Hoop Tensile

Hoop Tensile tests are used to measure compressive properties of the composite cylinders. As a result of this test method hoop tensile strength and material's stiffness values are obtained. The hoop tensile test was performed according to the ASTM D2290 standard.

A Shimadzu™ AGS-X universal testing machine with a maximum capacity of 100kN was used for apparent hoop tensile tests using a special split disc tester. The schematic representation of the test apparatus is shown in Figure 28.

$$\sigma_{hts} = \frac{F_{max}}{(2A_{min})} \quad (3.6)$$



Figure 28. Hoop tensile test setup.

### 3.1.3.2.3. Radial Compression

The radial compression test method is commonly used to obtain the compressive properties (like compressive strength and strain) and material's stiffness of composite materials according to ASTM D2412. A universal testing machine with a pressure

apparatus was used for the radial compression test at room temperature. The schematic representation of the radial compression test setup can be seen in Figure 29.

$$PS = \left(\frac{F}{\Delta y}\right) \quad (3.7)$$



Figure 29. Radial compression test setup.

#### **3.1.3.2.4. Thermal Test**

Thermal pipe conductivity tests could not be performed because the samples were not suitable for the test setups.

### **3.2. Finite Element Method**

This study's main objective is the numerical solution and prediction of the polymer composite structure's mechanical and thermal properties. For this purpose, engineering simulation software ANSYS 2022/R2 was used. Finite element analyses

were performed statically and thermally. The main toolboxes and test procedures are explained in the below titles. In the numerical analysis, the solid element type SOLID186 was used. Mesh convergence studies are not given in this thesis because of the quality of the element. 1 mm element size is used for all models, and the minimum element quality is greater than 0,40.

### 3.2.1. Analysis Tree

Finite element analysis is occurred by some steps to illustrate the test setup by numerically. This exemplification has an iterative solution of mathematical formulation in the software according to the boundary conditions of the system. To operate the analysis, firstly, composite structures should be identified to the system. This identification could made in separately or using ACP(PRE) toolbox to imply used materials, geometry, mesh model. If the analyze input parameters (like material and geometry) given separately at the end of the composite structure determination again ACP(PRE) toolbox should be used to identify composite structure. Sometimes separate identification can be useful for performing multiple analyzes on one analysis page. After these operations, composite structure should be assigned as fiber angle, fiber thickness and ply stack-ups. Subsequently the composite model determination, related analysis toolboxes are used for the execution of the test methods. At the end of the analysis, post analysis is executed by ACP(POST) for to predict the failure model of this composite structure. All these system connections are called as “Analysis Tree”. An example analysis tree is given in Figure 30.

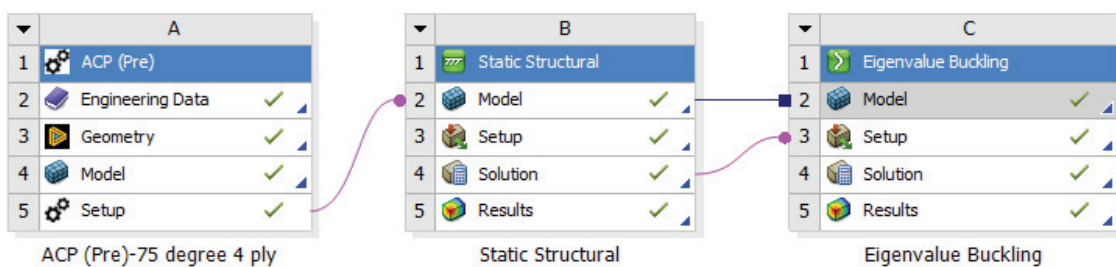


Figure 30. An example analysis tree in ANSYS.

### 3.2.2. ACP(PRE)

As previously mentioned in the above paragraph, ACP(PRE) is used to define composite layout. Identified materials and geometries are used in the setup tab to create composite ply materials and layup geometry. The Setup tab has several steps to define the composite structure. With these steps, materials and their properties, fiber direction, layup zone, layup direction, and modeled composite structure are defined in ACP(PRE). An example of a modeled composite structure in ACP(PRE) is shown in Figure 31.

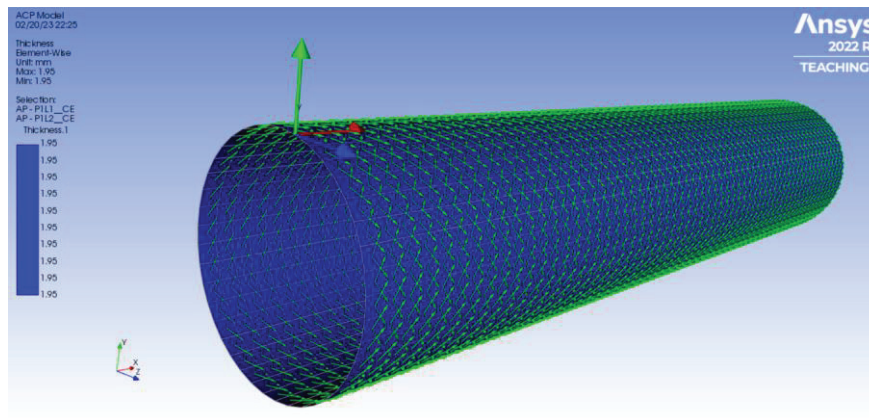


Figure 31. An example modelled composite structure in ACP(PRE).

When the modeling process of the composite material is completed, the test system definition phase is started at the appropriate interface.

### 3.2.3. Static Structural

The ANSYS Static Structural Toolbox provides a comprehensive set of tools for simulating static structural behavior, including linear and nonlinear material models, various types of elements, and a range of boundary conditions. One of the key features of the ANSYS Static Structural Toolbox is its ability to model and simulate composite materials, which are widely used in a variety of industries due to their high strength-to-weight ratio and other desirable properties. The toolbox allows users to simulate the

behavior of composite materials under different types of loads and analyze the impact of different design parameters on the material's performance. In addition, the ANSYS Static Structural Toolbox provides a range of post-processing capabilities, including visualization tools for displaying stress and strain results, displacement, and deformation, as well as tools for generating detailed reports and graphs. To perform a static three-point bending analysis, the "Static Structural" interface is used. The coordinate system of the test structure, connection parts, zone designations, boundary conditions, and requested outputs are defined in this section. A typical three-point bending test setup example is given in Figure 32.

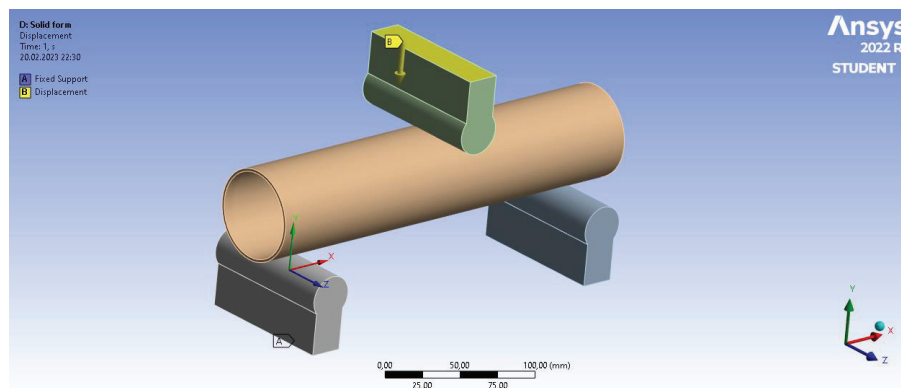


Figure 32. Three-point bending test setup illustration.

### 3.2.4. Steady-State Thermal

In the “Steady-State Thermal” tab, the interface is similar to the “Static Structural”. Yet, examination titles are different to “Static Structural”. With “Steady-State Thermal” analysis system, thermal property investigation can be examined.

The most important feature of the tool is its ability to predict the temperature distribution and thermal stresses in a system. It helps to identify potential hot spots or areas of thermal stress that may lead to failure or degradation of the system over time. By identifying these areas, engineers can make design modifications to improve the durability and reliability of the system. As an example, a test procedure demonstration is given in Figure 33.

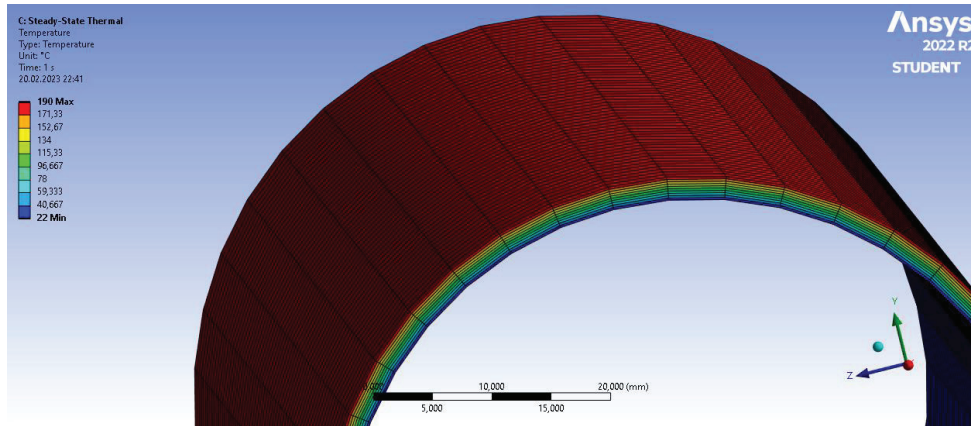


Figure 33. Thermal test demonstration.

### 3.2.5. ACP(POST)

At the end of the composite material finite element analysis, post-features of the structures are investigated in ACP(POST). In this part, post-forms of the composite materials' deformation and plies' crack formations are observed according to the failure criteria. Definitions and a solution image are given in Figure 34.

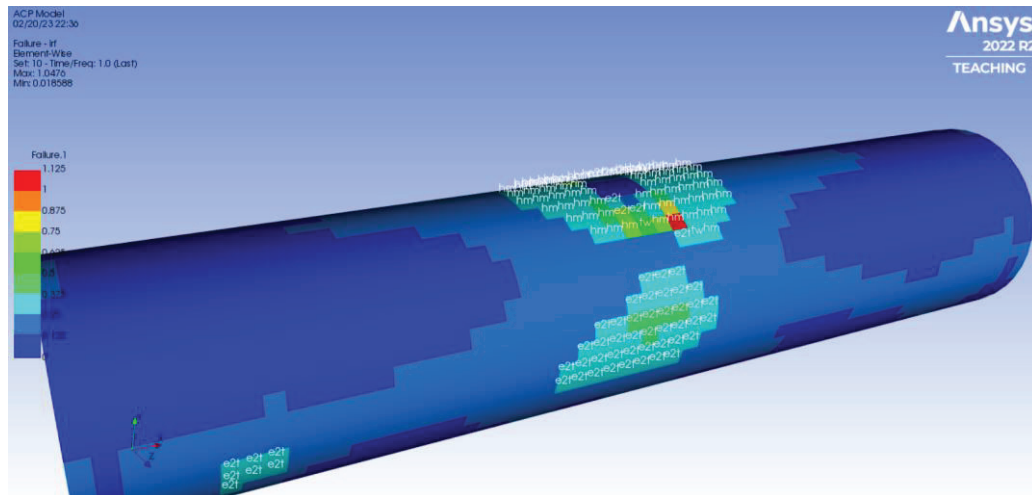


Figure 34. Post processing image of the test setup.

As an objective for investigating failure criteria for composite materials in ANSYS, ACP(POST) is used. Failure analyses are clearly more complex for composite

materials than for isotropic materials. This complexity occurs for some reasons, like orthotropic material behavior, different fiber properties, matrix properties, etc. In ANSYS, there are some failure criteria available to predict failure modes of composite materials. With this failure analysis in ACP(POST), it was aimed to understand the first-ply failure mode of the material. As a result of these analyses, the Inverse Reserve Factor value is obtained. The inverse reserve factor is equal to the ratio of ultimate load to ultimate strength. If the IRF value is greater than one, failure will occur. However, if the IRF value is less than 1, it is considered safe.

Given failure criteria in ACP are:

- Maximum Strain
- Maximum Stress
- Tsai-Wu
- Tsai-Hill
- Hashin
- Puck
- LaRC
- Cuntze
- Face Sheet Wrinkling
- Hoffman

Groups of these failure criteria are:

- Independent Failure Criteria
  - Maximum Stress
  - Maximum Strain
- Polynomial Failure Criteria
  - Tsai Hill
  - Tsai-Wu
  - Hoffman
- Direct Mode Failure Criteria
  - Hashin
  - Puck
  - LaRC
  - Cuntze

# CHAPTER 4

## RESULTS AND DISCUSSION

For the comparison of the results of experimental tests and numerical solutions, each test methods were illustrated numerically as similar as the experimental tests. Statistically solved numerical models' mechanical properties of the composite structures were predicted by failure criteria mechanisms. Four of the criteria were identified in the numerical analysis and these criteria are Maximum Stress, Maximum Strain, Tsai-Wu and Hashin criteria.

### 4.1. Material Properties

The materials' properties obtained from the produced composite plate parts are given in Table 15 according to the test standards. These values are used in the finite element analysis program to observe numerical calculations on Ansys for an exemplified experimental procedure. The polar properties of materials are given in Figures 35 as Carbon Epoxy and Carbon phenolic.

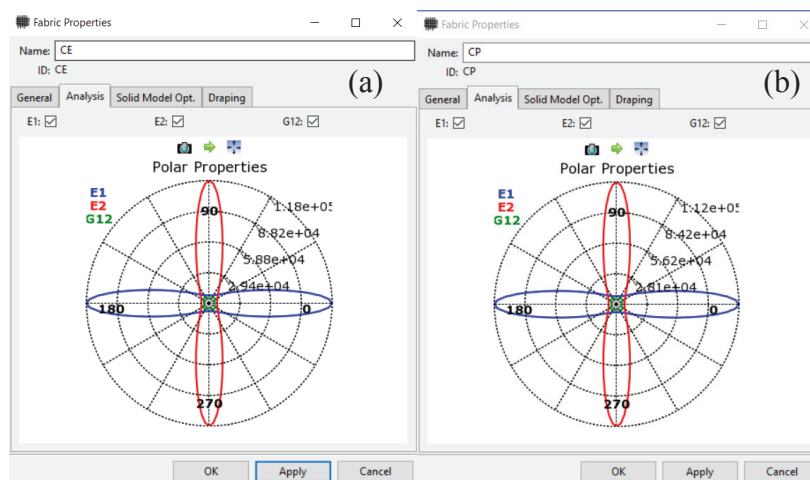


Figure 35. Polar properties of composite structures. (a) Carbon/Epoxy, (b) Carbon/Phenolic.

Table 14. Composite materials' properties that are used in the ANSYS FEM program.

Symbol	Description	Unit	Carbon Fiber / Epoxy Value	Carbon Fiber / Phenolic Value
$E_1$	Longitudinal Modulus (Fiber Dominated)	MPa	117560	112320
$E_2 = E_3$	Transverse Modulus (Matrix Dominated)	MPa	7610	7390
$\nu_{12} = \nu_{13}$	Poisson's Ratio (In-Plane)		0,28	0,27
$\nu_{23}$	Poisson's Ratio (Plane 2-3)		0,4	0,42
$G_{12} = G_{13}$	Shear Modulus (In-Plane)	MPa	4860	4700
$G_{23}$	Shear Modulus (Plane2-3)	MPa	2910	3050
$X_t$	Longitudinal Tensile Strength (Fiber Dominated)	MPa	1573	1544
$X_c$	Longitudinal Compressive Strength (Fiber Dominated)	MPa	-682	-610,36
$Y_t$	Transverse Tensile Strength (Matrix Dominated)	MPa	32,5	28,77
$Y_c$	Transverse Compressive Strength (Matrix Dominated)	MPa	-61	-65,3
$S_{12}$	Shear Strength (In-Plane)	MPa	73	68,21
$k'$	Thermal Conductivity	W/mK	3,322	4,073

## 4.2. FEM Test Models and Results

In the finite element analyses, used composite cylinders were modeled similar to the produced filament wound cylinders as 55-degree winding angle, 60 mm inner diameter, and 61.95 outer diameter which have a 1.95 mm composite thickness. Different lengths are used in the analyses as the test type that the standards suggested dimensions. These dimensions are shown in each test explanation title with technical drawings. As a result of the tests performed statically, the values of the composite structure experimentally sought were obtained.

### 4.2.1. Three Point Bending

Modeling of the three-point bending analyses in Ansys include a 300-mm-long pipe which has a 1.95 mm composite thickness for both composite pipes. The course dimensions of the pipes' technical drawings are given in Figure 36.

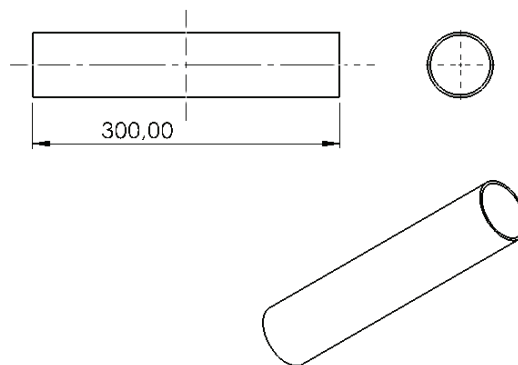


Figure 36. Three Point Bending test specimen technical drawing.

The boundary conditions of three-point bending tests are implemented as a 250 mm bottom support span length and mid-span at the mid-point of the pipes. In this support placement, the bottom supports are fixed, and top support has a displacement to interact with the force on the composite cylinder. The conclusion of the movement of the top support, the analysis performed, and the resultant stress and strength values are observed.

The amount of displacement was renewed with several tests to get close to the “Inverse Reserve Factor” value is one. Experimentally and numerically modeled boundary conditions are shown in Figure 37.

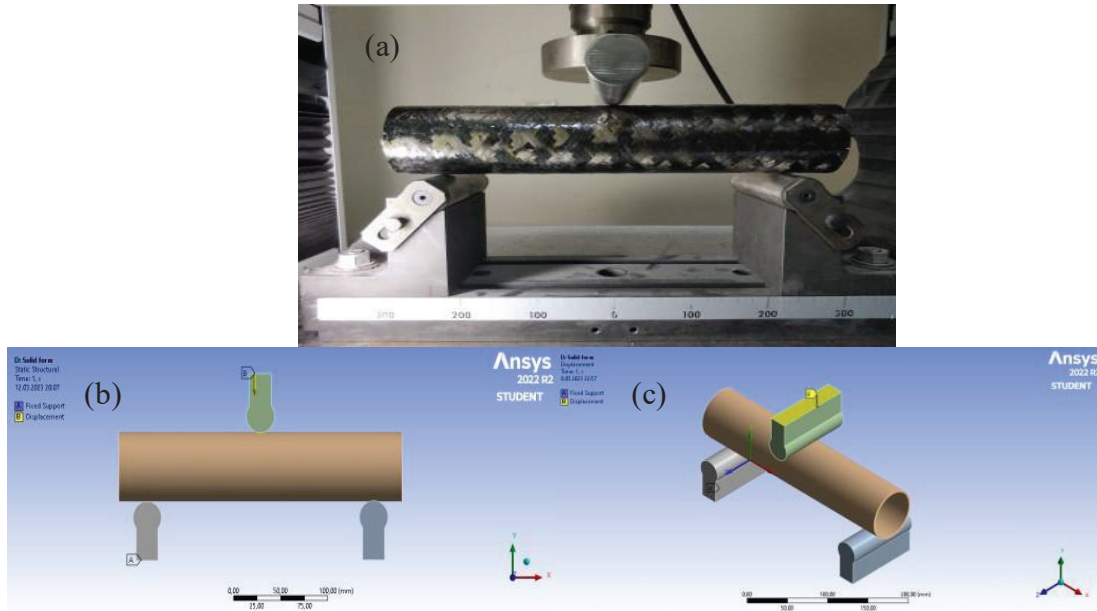


Figure 37. Three Point Bending analysis boundary conditions. (a) experimental, (b) front side FEM and (c) isometric view FEM.

As a result of the FEM analysis, the strength value of the pipes was obtained with the help of the first ply failure theory on Ansys. The composite tool was used to find the “Inverse Reserve Factor” to predict when the first ply failure will start, and which ply of the composite will fail. With this operation, the IRF value gave to the strength value of the composite pipe.

While the IRF value is found with this theory, Ansys gives the failed ply number, failure direction and type of loading at failure. These predictions validated by the experimental testes. Resultant stress values and IRF illustrations are given in Figure 38 and Figure 39.

After all the numerical analysis, the flexural strengths of the two differently wound composite structures were obtained as 233.54 MPa for five-layer Carbon/Epoxy wound composite cylinder and 235.67 MPa for four-layer Carbon/Epoxy and one-layer Carbon/Phenolic wound composite cylinder. The difference between these two structures

were found as -5.10%. If the comparison of experimental and numerical results is calculated as -7.21% for five-layer Carbon/Epoxy filament wound composite cylinder and -11.66% for four-layer Carbon/Epoxy and one-layer Carbon/Phenolic composite cylinder.

According to the failure mechanism, first ply failure was observed e2c. e2c means that failure starts at maximum point of the cylinder as second direction and compression force in accord with maximum strain and Tsai-Wu failure criteria. This first ply failure is same for both composite structures.

The differences between the experimental and FEM results for three-point bending tests are shown graphically in Figure 40.

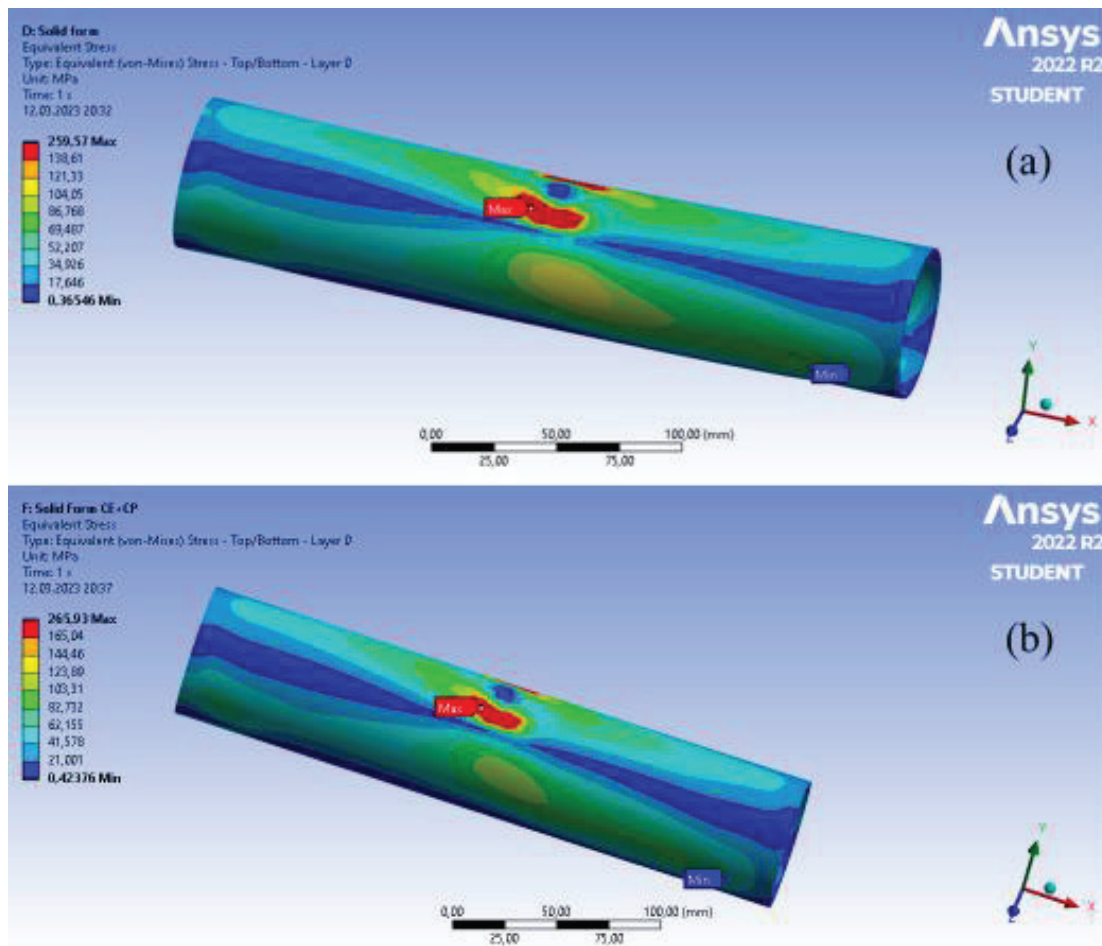


Figure 38. Three Point Bending FEM analyses stress results. (a) 5-layer Carbon/Epoxy pipe, (b) 4-layer Carbon/Epoxy and 1-layer Carbon/Phenolic composite pipe.

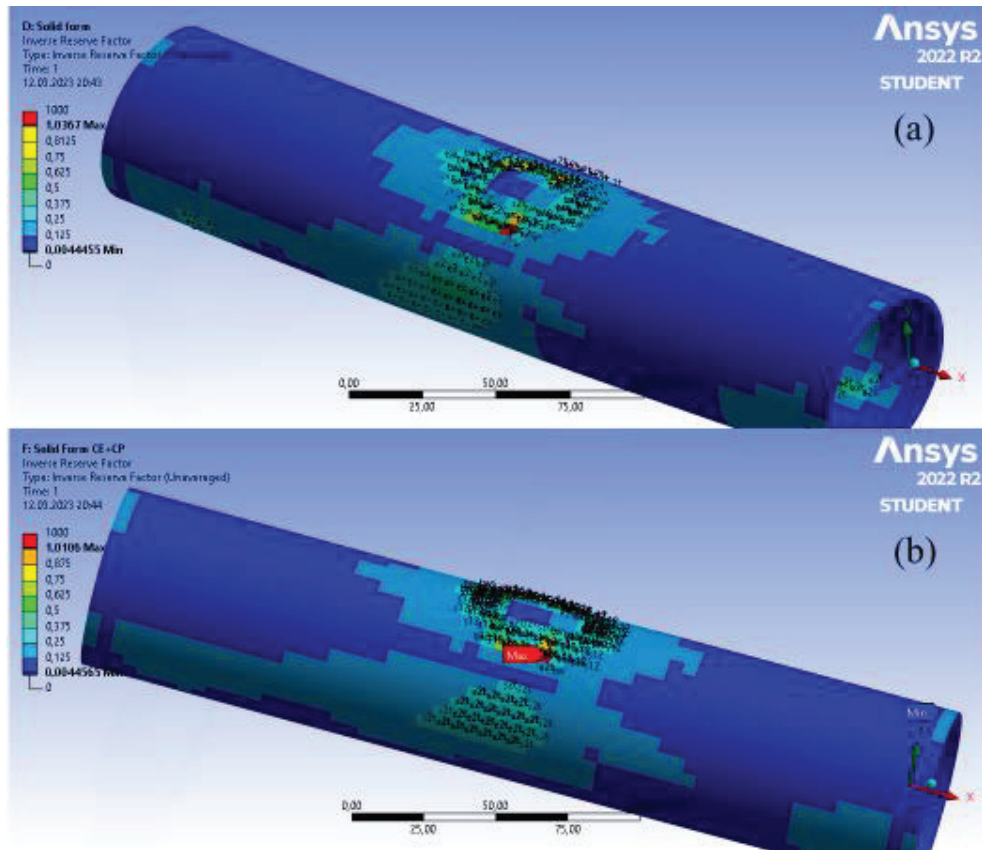


Figure 39. Three Point Bending FEM analyses failure analyses results. (a) 5-layer Carbon / Epoxy pipe, (b) 4-layer Carbon / Epoxy and 1-layer Carbon / Phenolic composite pipe.

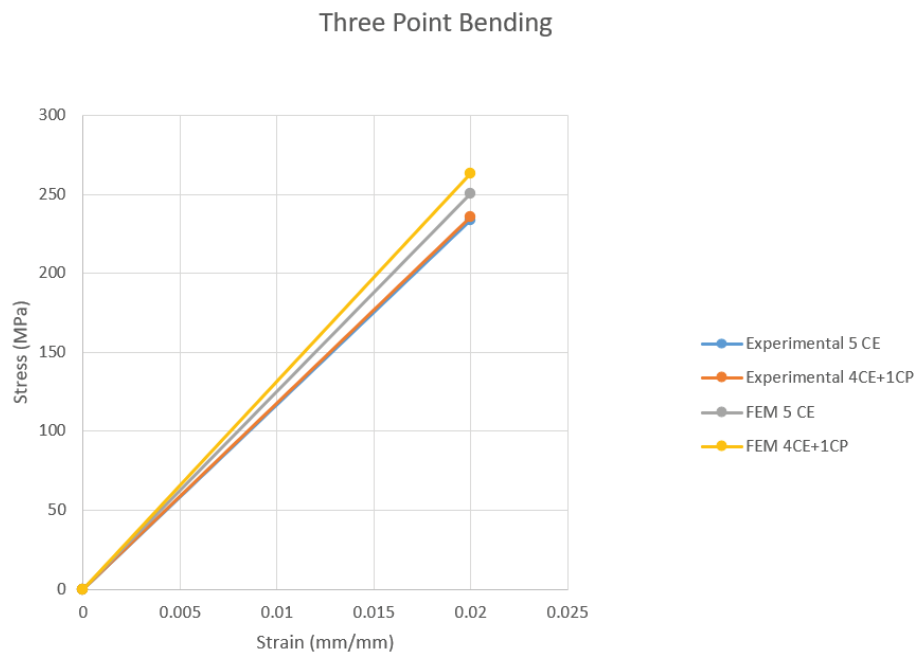


Figure 40. Three Point Bending Analysis Stress-Strain graph.

## 4.2.2. Hoop Tensile

In Hoop Tensile test method, average produced material dimensions are used for modeling part and the specified test dimensions are given in Figure 41 as a technical drawing. These dimensions are related to the ASTM standard that is used in experimental tests. Also, the boundary conditions and support materials are modeled on Ansys according to the ASTM D2290 standard.

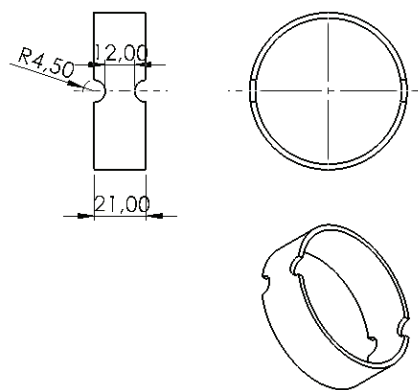


Figure 41. Hoop Tensile test specimen technical drawing.

Identified boundary conditions occurs in two main parts as lower support is not allowed to move or rotate in any direction, and other boundary condition is that the upper support moves in the +y direction till the maximum composite strength value is obtained. To show clearer the applied conditions main locations are shown in Figure 42 with a divided support picture.

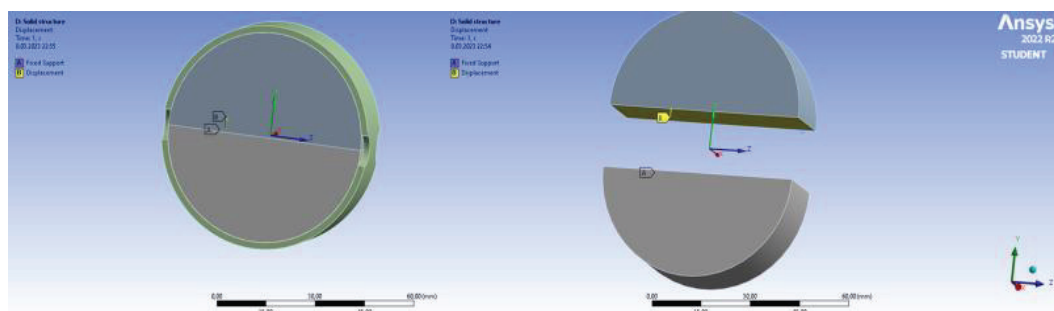


Figure 42. Hoop Tensile analysis boundary conditions.

As a result of the upper support movement in the +y direction, hoop tensile strength was obtained on Ansys. Prediction and calculation of the composite structure failure are used to find the strength value achieved with a similar method with three-point bending analyses. Composite structure hoop tensile strength was found by failure conditions on post-processes. Hoop tensile tests' numerical results were obtained as 475,59 MPa for five-layer Carbon/Epoxy structure and 477.83 MPa for four-layer Carbon/Epoxy and one-layer Carbon/Phenolic structured composite cylinder. The difference between five-layer Carbon/Epoxy filament wound cylinder and four-layer Carbon/Epoxy and one-layer Carbon/Phenolic filament winding structure was observed as 3.99%. According to these results, the difference between experimental and numerical methods were observed as -3.04% for five-layer Carbon/Epoxy composite and 1.54% for four-layer Carbon/Epoxy and one-layer Carbon/Phenolic composite cylinder. At the end of the analysis's failure was observed as e2t for both composite structures according to the post processing of the software. Resultant stress and inverse reserve factor values are given in Figures 43 and 44. The differences between the experimental and FEM results for Hoop Tensile tests are visually shown in Figure 45.

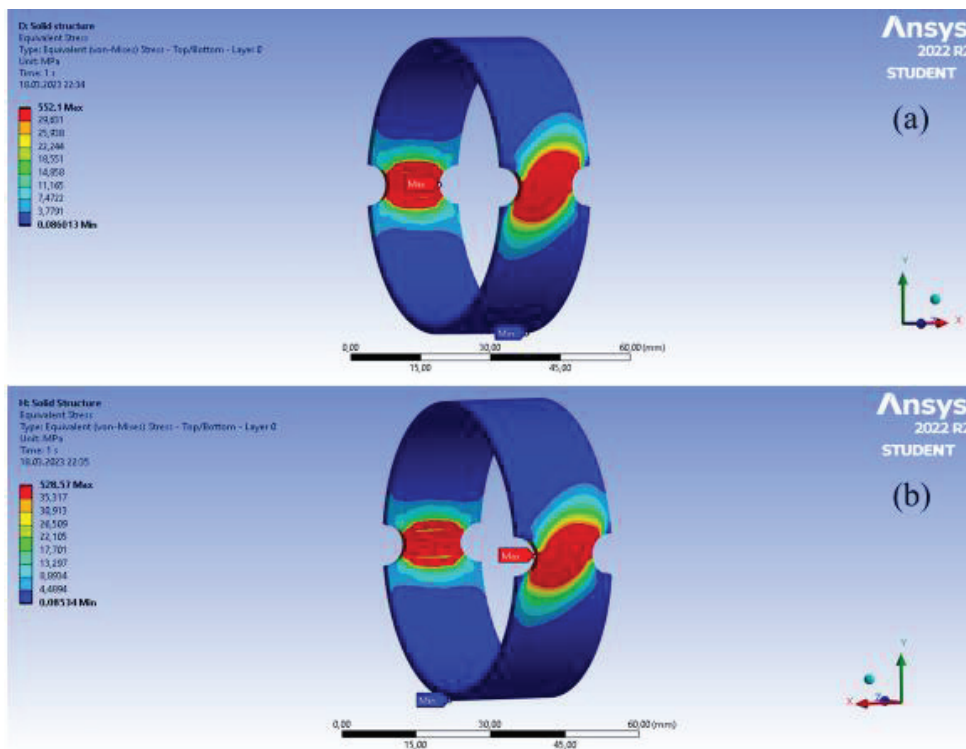


Figure 43. Hoop Tensile FEM analyses stress results. (a) 5-layer Carbon / Epoxy pipe, (b) 4-layer Carbon / Epoxy and 1-layer Carbon / Phenolic composite pipe.

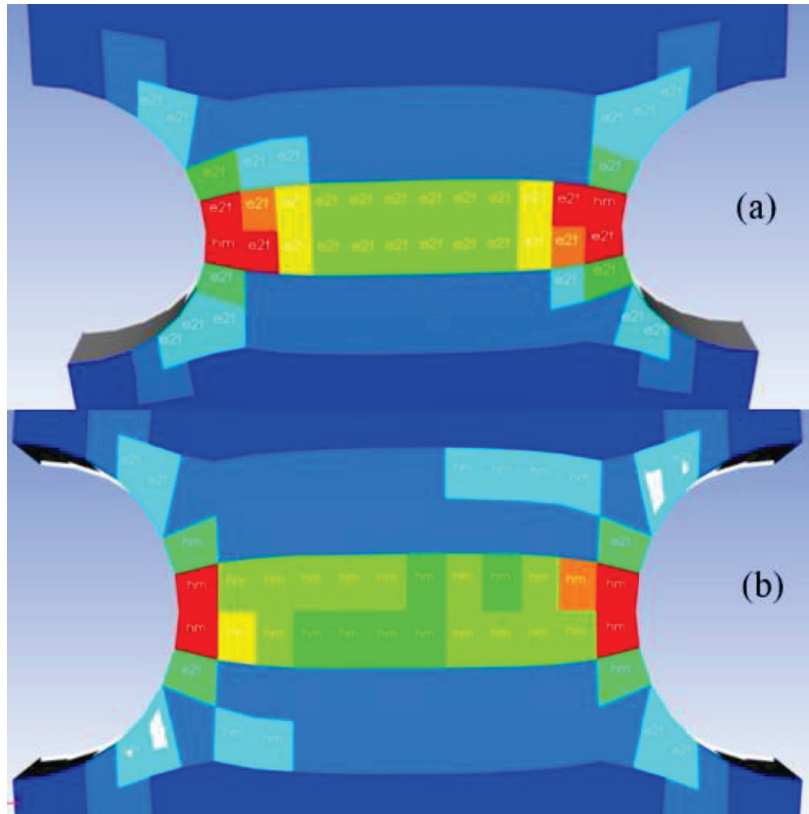


Figure 44. Hoop Tensile FEM analyses failure analyses results. (a) 5-layer Carbon / Epoxy pipe, (b) 4-layer Carbon / Epoxy and 1-layer Carbon / Phenolic composite pipe.

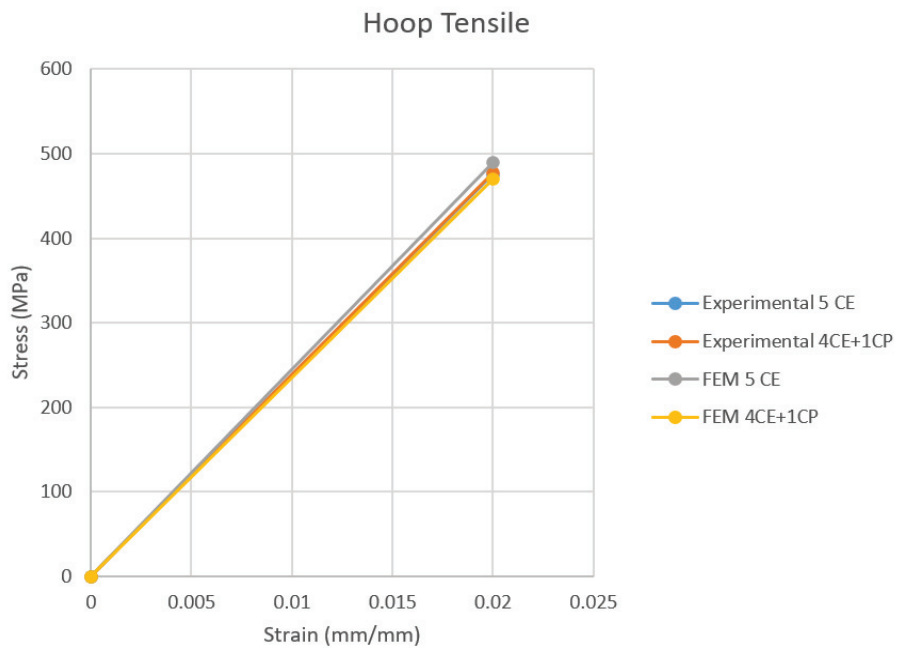


Figure 45. Hoop Tensile Analysis Stress-Strain graph.

### 4.2.3. Radial Compression

According to the produced test materials' average dimensions are used in the FEM analyses and these dimensions of the analyzed materials are given in Figure 46.

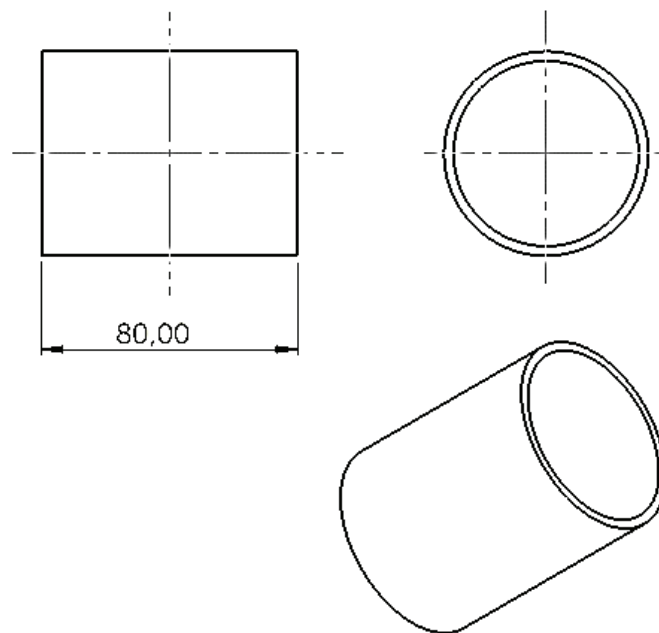


Figure 46. Radial Compression test specimen technical drawing.

The boundary conditions of the radial compression analysis of the composite cylinders are occurred by two plates that are parallel to each other and composite specimen that are produced to the desired dimensions. This composite cylinder assumed that touching every point of the plates was entirely a line. The lower plate is assumed to be a fixed plate that has no movement in any direction. The upper plate is moving along the -y direction. With these analyses of the composite cylinder, which is perpendicular to the plates, stiffness values are obtained. The compressive stiffness of the composite structure and behavior of the deformation (failure behavior) can be observed with this test method.

An illustration of the boundary condition of the analysis model is shown in Figure 47.

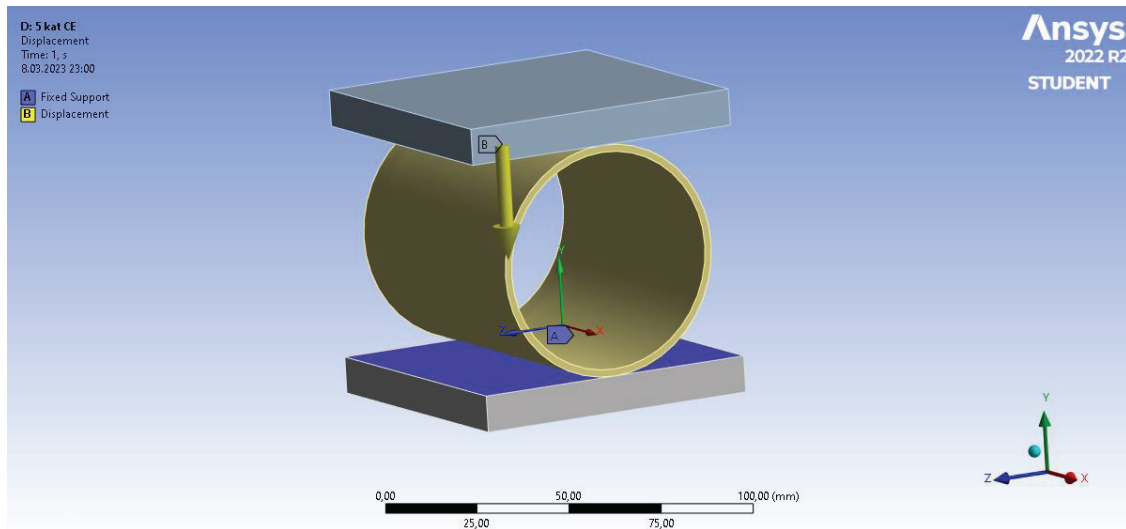


Figure 47. Radial compression analysis boundary conditions.

As a result of the analyses, applied force values (N) and strain values in the y axis (mm/mm) are achieved to obtain stiffness values as kN according to the ASTM D2412 standard. The IRF values of the analyses performed are shown in Figure 4.13.

The results were obtained by statistically solved analysis as 490.93 N/mm for five layers of Carbon/Epoxy composite cylinder and 488.71 N/mm for four layers Carbon/Epoxy and one layer Carbon/Phenolic filament wound composite cylinder. The first ply failure observed as e2c, which means the compressive strength in direction two according to the maximum strain failure criteria in ANSYS. This criterion showed the inner layer of the composite structures fails first.

The difference between both finite element analyses of two types of composite cylinders is 0.45%. When the analysis results are compared with experimental results the difference between these two methods, -6.15% difference was observed for a five-layer Carbon/Epoxy composite cylinder, and -3.53% differences were observed for a four-layer Carbon/Epoxy and one layer Carbon/Phenolic wound cylinder.

According to the failure analyses, failure occurs at given forces according to the Maximum Stress criteria. View of post process results are shown in the Figure 48.

The differences between the experimental and FEM results for Radial Compression tests are shown in the Figure 49.

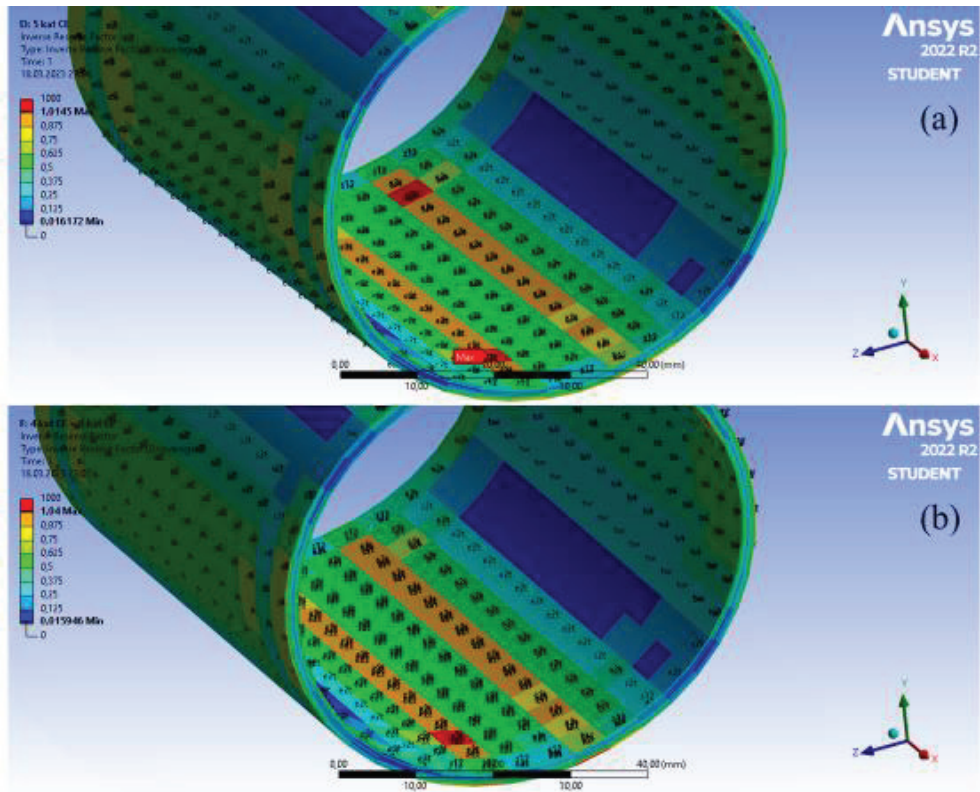


Figure 48. Radial Compression FEM analyses failure analyses results. (a) 5-layer Carbon / Epoxy pipe, (b) 4-layer Carbon / Epoxy and 1-layer Carbon / Phenolic composite pipe.

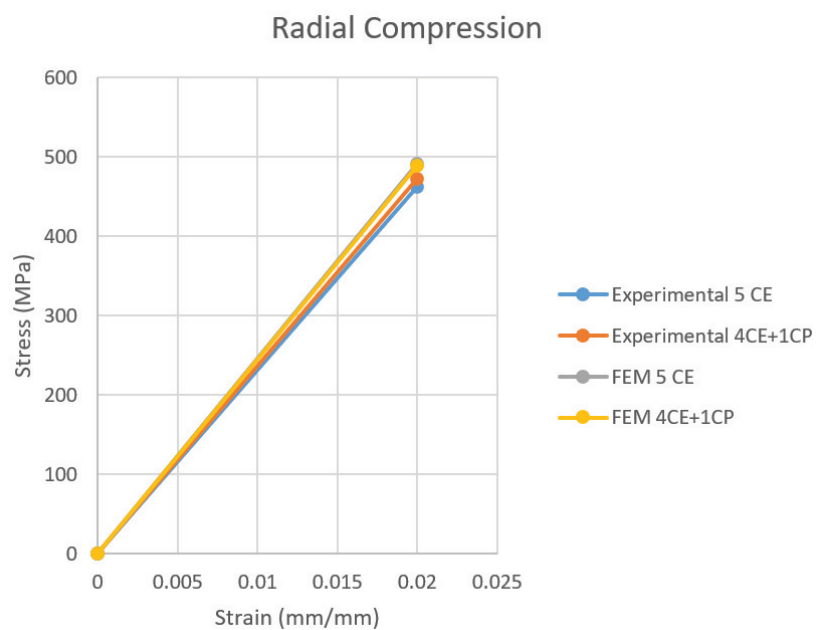


Figure 49. Radial Compression Analysis Stress-Strain graph.

#### 4.2.4. Thermal Analysis

In this study, thermal analyses couldn't be performed both experimentally and numerically because of the experimental equipment's inability to observe cylindrical samples for the analytical material identification. Only thermal conductivity was observed experimentally for plates. However, this conductivity value does not represent hundred percent true values for the Carbon/Epoxy and Carbon/Phenolic materials due to the unsuitable sample shape for the KEM QTM 500 test machine. Even though, obtained conductivity values are used in the numerical modeling material information.

With these values, there are no extinct resultant outputs on the analyses, yet the thermal distribution for each ply examined for the outer degree is 190 Celsius and 22 Celsius for the inner degree. The boundary conditions and test results are given in Figures 50 and 51 respectively. It was observed that the heat transfer between the Carbon/Epoxy layers had a change of  $\pm 17$  to 16.43 degrees, while a heat transfer of 13.9 degrees was observed in the Carbon/Phenolic layer. When this difference was calculated, a thermal insulation of 15.4% was observed compared to Carbon/Epoxy tube.

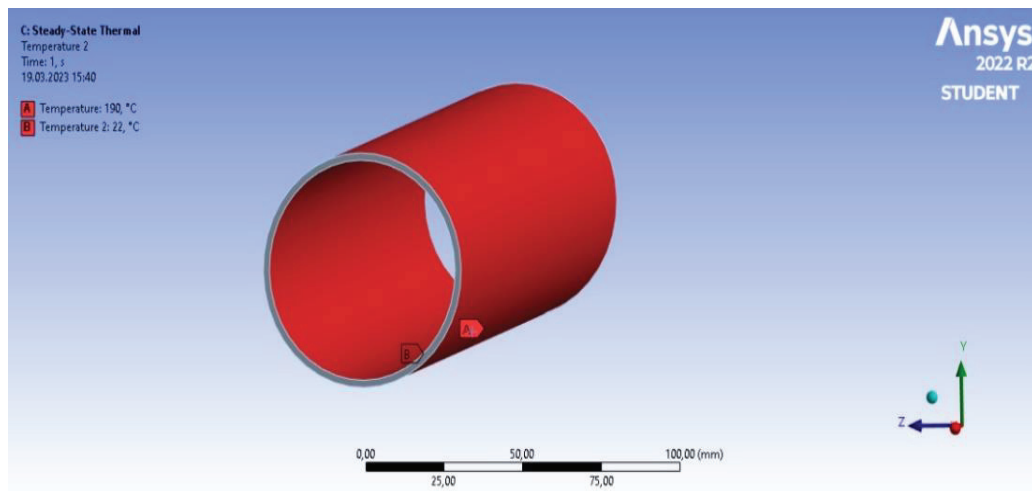


Figure 50. Thermal boundary conditions of modelled analyses.

As a result of this study, obtained all values and differences are given in the Table 15 and 16.

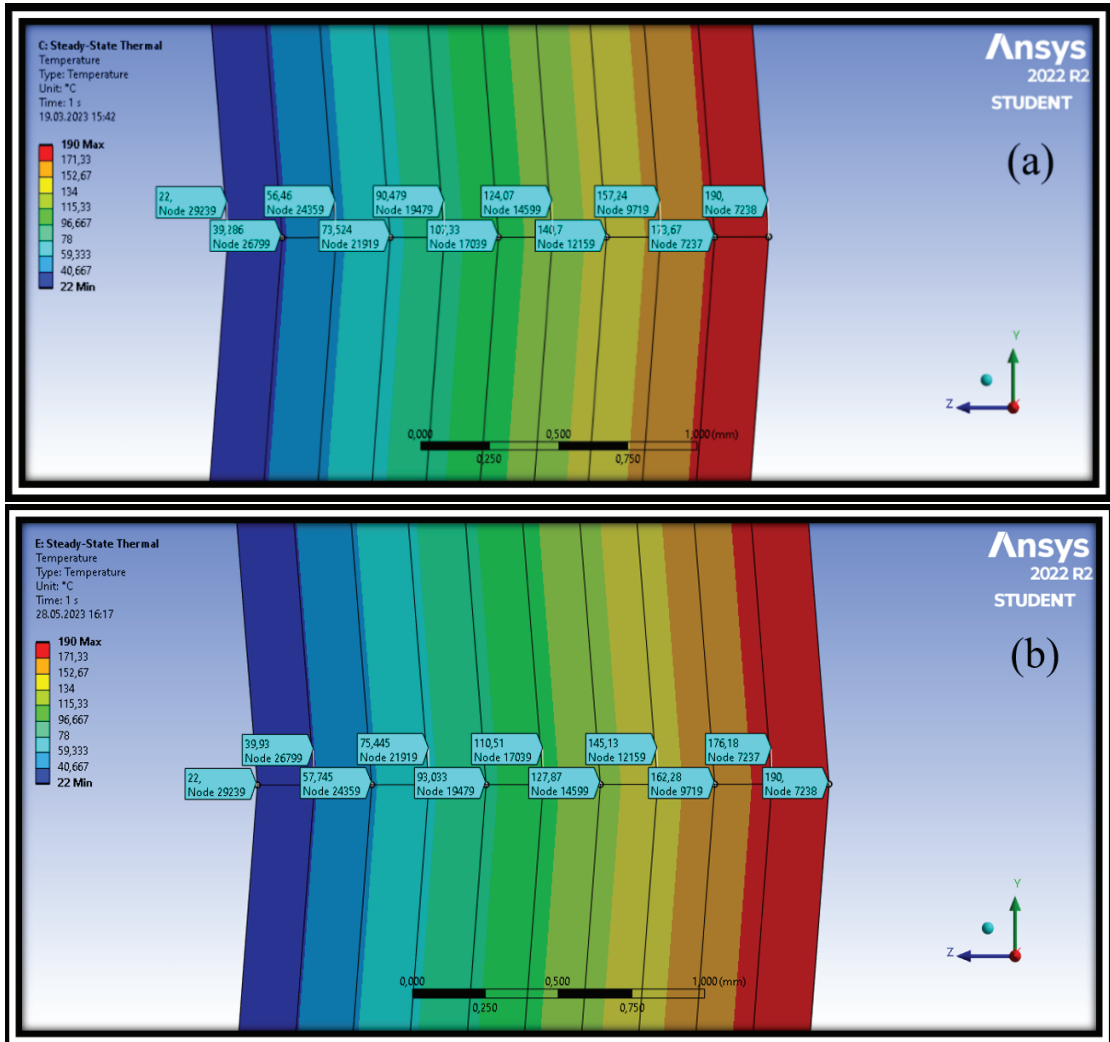


Figure 51. Thermal Conductivity FEM analyses failure analyses results. (a) 5-layer Carbon / Epoxy pipe, (b) 4-layer Carbon / Epoxy and 1-layer Carbon / Phenolic composite pipe.

Table 15. Results of experimental test and finite element analysis.

Resultant Table	Experimental		Numerical (FEM)	
	5 Layer Carbon/Epoxy	4 Layer Carbon/Epoxy + 1 Layer Carbon/Phenolic	5 Layer Carbon/Epoxy	4 Layer Carbon/Epoxy + 1 Layer Carbon/Phenolic
Three-Point Bending Test Bending Strength (MPa)	233.54	235.67	250.38	263.14
Radial Compression Test Pipe Stiffness (N/mm)	462.46	472.06	490.93	488.71
Hoop Tensile Test Hoop Tensile Strength (MPa)	475.59	477.83	490.06	470.47

Table 16. Differences and error rates of all methods and tests.

Differences Table	Experimental	Numerical (FEM)	Experimental vs FEM error rate	
			5 Layer Carbon/Epoxy	4 Layer Carbon/Epoxy + 1 Layer Carbon/Phenolic
Three-Point Bending Test Bending Strength (%)	±0.91	±5.0963	±7.21	±11.66
Radial Compression Test Pipe Stiffness (%)	±2.08	±0.45	±6.15	±3.53
Hoop Tensile Test Hoop Tensile Strength (%)	±0.47	±3.99	±3.04	±1.54

## CHAPTER 5

### CONCLUDING REMARKS

As a conclusion of this study, composite materials, filament winding technique, testing the produced specimens, standards of the tests, and the main objective finite element modeling technique topics were examined to perform more reliable and exact predictions by the finite element modeling technique.

The main objective of the thesis is to investigate the finite element models to obtain the strengths of the composite cylinders according to the three mechanical and one thermal testing methods. For this purpose, modeling a precise composite structure in the analysis program Ansys is an important point of the thesis. This modelling illustrates the excellent product of the artificial world. Also, it was tried to show the possibility and effectiveness of the matrix hybridization process.

The obtained results of the analysis were criticized with experimental results to show how accurate the modeled test systems in the Ansys. In mechanical tests, the results were clearly compared to each other as a finite element model and experimentally produced composite cylinders. The comparison results showed the accuracy of the differences between the two models shown. These values changed according to test methods, and the maximum error rate shown in the three-point bending test as %11.66. All test methods' results showed different percentages of differences. However, the differences between five-layer Carbon/Epoxy composite cylinders and four-layer Carbon/Epoxy + one-layer Carbon/Phenolic composite cylinders were shown in a fewer difference between each other.

When the results are criticized, this change would be occurred by the diamond shapes and distributions' effect on the composite cylinders. While the cylinder is produced by the filament winding machine, continuous fiber winding poles affect the diamond shapes in terms of dimensions and amounts. All of the composite cylinders were produced with the same production parameters. Nevertheless, while the cylinder is modeling in Ansys, the winding operation is carried out as a full layer. It means that in the finite element model, there is no diamond shape, and every point of the composite

structure shows a similar behavior. These diamond-shape differences may have made a big difference among test methods.

To sum up, it was clearly shown that the finite element analyses have some limitations in performing test models entirely similar to the production of filament-wound composite cylinders, but close prediction of strength and desired property values can be obtained in a realistic way. Even if all situations were not the same for these two methods, prediction of the necessary feature could be obtained by the finite element modeling method. Also, it was learned from this study that chemical reaction possibilities should not be ignored for matrix hybridization studies.

As a future work of this study,

- Suitable thermal test machines can be used.
- The thermal behavior can be observed by passing hot water through the pipe and placing probes between each layer.
- The predictions observed with static analysis can be made with dynamic analysis, and the difference between the static analysis prediction and dynamic analysis results can be compared.
- It can be observed that by making the thermal conduction outer coating, the difficulty in production is reduced, and thus the effects are increased.

## REFERENCES

- Clyne, T. W., & Hull, D. 2019. "An Introduction to Composite Materials. In An Introduction to Composite Materials." <https://doi.org/10.1017/9781139050586>
- Chung, D. D. L. 2010. "Composite Materials." <https://doi.org/10.1007/978-1-84882-831-5>
- ŠERIFI, V., Tarić, M., JEVTIĆ, D., Ristovski, A., & ŠAHINAGIĆ–ISOVIĆ, M. 2018. "Historical development of composite materials."
- Harris, B. 1999. "ENGINEERING COMPOSITE MATERIALS."
- Kangal, Serkan. 2019. "Modeling, Simulation and Analysis of Type-III Composite Overwrapped Pressure Vessels for High-Pressure Gas Storage." Order No. 28472588, Izmir Institute of Technology (Turkey).
- Balya, Bora. 2004. "Design and Analysis of Filament Wound Composite Tubes." M.S.- Master of Science, Middle East Technical University.
- Ma, Q., Kumar, N. M., Quanjin, M., Rejab, R. M., & Zhang, B. 2019. "Filament winding technique: SWOT analysis and applied favorable factors Water based photovoltaic systems (WPVS): Floating and Submerged PV View project Composite Sandwich Panel with Novel Contoured Core View project Filament Winding Technique: SWOT Analysis and Applied Favorable Factors."
- J. Ramkumar, 2017 "Manufacturing of Composites: Lecture 9 notes", Indian Institute of Technology Kanpur.
- Rao, S. S. 2017. "The finite element method in engineering." Butterworth-Heinemann.
- Kartav, Osman. 2020. "Design and Production of Light-Weight Pressure Resistant Composite Tank Materials and Systems for Hydrogen Storage." Order No. 29079066, Izmir Institute of Technology (Turkey).

- Potter, Kevin 1996. "An Introduction to Composite Products: Design, Development and Manufacture." Springer, 5th Ed. Chapman & Hall, London.
- Abdallah, M. H., & Braimah, A. 2022. "Numerical design optimization of the fiber orientation of glass/phenolic composite tubes based on tensile and radial compression tests." *Composite Structures*, 280. <https://doi.org/10.1016/j.compstruct.2021.114898>
- Arslan Özgen, G., Yüçetürk, K., Tanoğlu, M., & Aktaş, E. 2019. "An Investigation on Hybrid Composite Drive Shaft for Automotive Industry."
- Toh, W., Tan, L. bin, Tse, K. M., Giam, A., Raju, K., Lee, H. P., & Tan, V. B. C. 2018. "Material characterization of filament-wound composite pipes." *Composite Structures*, 206, 474–483. <https://doi.org/10.1016/j.compstruct.2018.08.049>
- Gunasegaran, V., Prashanth, R., & Narayanan, M. 2013. "Experimental investigation and finite element analysis of filament wound GRP pipes for underground applications." *Procedia Engineering*, 64, 1293–1301. <https://doi.org/10.1016/j.proeng.2013.09.210>
- Maziz, A., Tarfaoui, M., Gemi, L., Rechak, S., & Nachtane, M. 2021. "A progressive damage model for pressurized filament-wound hybrid composite pipe under low-velocity impact." *Composite Structures*, 276. <https://doi.org/10.1016/j.compstruct.2021.114520>
- Zacharakis, I., Giagopoulos, D., Arailopoulos, A., & Markogiannaki, O. 2022. "Optimal finite element modeling of filament wound CFRP tubes." *Engineering Structures*, 253. <https://doi.org/10.1016/j.engstruct.2021.113808>
- Uz, Y. C. 2021. "Development and Characterization of Innovative Fiber Reinforced Prepregs and Their Composites Containing Functional Fillers" (Doctoral dissertation, Izmir Institute of Technology (Turkey)).
- Aydın, M. 2019. "Development of Fiber Reinforced Cylindrical Composite Structures by Filament Winding Technique." (Master's dissertation, Izmir Institute of Technology (Turkey)).
- Rafiee, R., & Abbasi, F. 2020. "Numerical and experimental analyses of the hoop tensile strength of filament-wound composite tubes." *Mechanics of Composite Materials*, 56, 423-436.

- Li, J., Dong, C., & Chen, S. 2009. "Consolidation and warpage deformation finite element analysis of filament wound tubes." *Applied Composite Materials*, 16, 307-320.
- Kangal, S., Kartav, O., Tanoğlu, M., Aktaş, E., & Artem, H. S. 2020. "Investigation of interlayer hybridization effect on burst pressure performance of composite overwrapped pressure vessels with load-sharing metallic liner." *Journal of Composite Materials*, 54(7), 961-980.
- Kartav, O., Kangal, S., Yüçetürk, K., Tanoğlu, M., Aktaş, E., & Artem, H. S. 2021. "Development and analysis of composite overwrapped pressure vessels for hydrogen storage." *Journal of Composite Materials*, 55(28), 4141-4155.
- Stabla, P., Lubecki, M., & Smolnicki, M. 2022. "The effect of mosaic pattern and winding angle on radially compressed filament wound CFRP composite tubes." *Composite Structures*, 292, 115644.  
<https://doi.org/10.1016/j.compstruct.2022.115644>
- Reddy, R. P. K., Prabhu, M., & Ali, K. A. 2022. "A review on investigation of compressive load and buckling load on composite pipe for windmill application." *Materials Today: Proceedings*, 51, 1026-1029.  
<https://doi.org/10.1016/j.matpr.2021.07.081>
- Özbek, Ö., Doğan, N. F., & Bozkurt, Ö. Y. 2020. "An experimental investigation on lateral crushing response of glass/carbon intraply hybrid filament wound composite pipes." *Journal of the Brazilian Society of Mechanical Sciences and Engineering*, 42, 1-13.
- Masoumi, M., Abdellahi, S. B., & Hejazi, S. M. 2022. "Investigation flexural behavior of hybrid-reinforced layered filament wound pipes using experimental tests and numerical model." *Journal of Industrial Textiles*, 51(3\_suppl), 5219S-5242S.
- Asyraf, M. R. M., Ishak, M. R., Syamsir, A., Amir, A. L., Nurazzi, N. M., Norrahim, M. N. F., ... & Razman, M. R. 2023. "Filament-wound glass-fibre reinforced polymer composites: Potential applications for cross arm structure in transmission towers." *Polymer Bulletin*, 80(2), 1059-1084.